Comparative genomics of *Pseudomonas syringae* reveals convergent gene gain and loss associated with specialisation onto cherry (*Prunus avium*)

Michelle T. Hulin[1,4], Andrew D. Armitage[1], Joana G. Vicente[2], Eric B. Holub[2], Laura Baxter[2], Helen J. Bates[1], John W. Mansfield[3], Robert W. Jackson[4] and Richard J. Harrison[1,4]

1. NIAB EMR, New Road, East Malling, ME19 6BJ
2. School of Life Sciences, University of Warwick, Warwick Crop Centre, Wellesbourne, CV35 9EF
3. Faculty of Natural Sciences, Imperial College London, London SW7 2AZ, UK
4. School of Biological Sciences, University of Reading, Reading, RG6 6AJ, U.K

Corresponding author – richard.harrison@emr.ac.uk

Running head – Comparative genomics of *Pseudomonas* from cherry

Word count: 6500
Introduction: 762
Methods: 1040
Results: 2958
Discussion: 1661
Acknowledgements: 79

Figures: 8 (all colour)
Tables: 4
Supplementary information includes 24 figures, 26 tables and supplementary methods

Summary (200 words)

- Genome-wide analyses of the effector- and toxin-encoding genes were used to examine the phylogenetics and evolution of pathogenicity amongst diverse strains of *Pseudomonas syringae* causing bacterial canker of cherry (*Prunus avium*) including pathovars *P.s* pv. *morsprunorum* (*Psm*) races 1 and 2, *P.s* pv. *syringae* (*Pss*) and *P.s* pv. *avii*.
- Genome-based phylogenetic analyses revealed *Psm* races and *P.s* pv. *avii* clades were distinct and were each monophyletic, whereas cherry-pathogenic strains of *Pss* were interspersed amongst strains from other host species.
- A maximum likelihood approach was used to predict effectors associated with host specialisation on cherry. *Pss* possesses a smaller repertoire of type III effectors but has more toxin biosynthesis clusters compared with *Psm* and *P.s* pv. *avii*. Evolution of cherry pathogenicity was correlated with gain of genes such as *hopAR1* and *hopBB1* through putative phage transfer and horizontal transfer, respectively. By contrast, loss of the *avrPto/hopAB* redundant effector group was observed in cherry-pathogenic clades. Ectopic expression of *hopAB* and *hopC1* triggered the hypersensitive reaction in cherry leaves, confirming computational predictions.
- Cherry canker provides a fascinating example of convergent evolution of pathogenicity that is explained by the mix of effector and toxin repertoires acting on a common host.

Key words- avirulence, bacterial canker, comparative genomics, host specialisation, prediction, *Pseudomonas*, toxins, type III effectors

Introduction

Pseudomonas syringae is a species complex, associated with plants and the water cycle, comprising several divergent clades that frequently recombine (Young, 2010; Berge *et al.*, 2014; Baltrus *et al.*, 2017). Currently, thirteen phylogroups, based on Multi-Locus Sequence Typing (MLST), have been described (Parkinson *et al.*, 2011). As a plant pathogen, it is globally important, causing disease on over 180 different host species. *P. syringae* is responsible for recurring chronic diseases in perennial crops, such as cherry canker (Lamichhane *et al.*, 2014), and also sporadic outbreaks on annual crops, such as bacterial speck of tomato (Şahin, 2001). Individual strains are highly specialised and assigned to over 60 host-specific pathovars; some of these are further divided into races which show host genotype specificity (Joardar *et al.*, 2005). This makes *P. syringae* an important model to study the evolution of host specificity (O'Brien *et al.*, 2011; Mansfield *et al.*, 2012).

High-throughput sequencing has become a major tool in bacterial studies (Edwards & Holt, 2013). With the increasing number of genomes available, population-level studies can now be conducted to ask complex evolutionary questions, such as how disease epidemics emerge and what ecological processes drive the evolution of pathogenicity (Guttman *et al.*, 2014; Monteil *et al.*, 2016). Before genomic methods were available, mutational studies of *P. syringae* were used to identify functional virulence factors in pathogenesis, such as type III secretion system effector (T3E) repertoires and toxins (Lindgren 1997; Bender *et al.* 1999). Some T3Es were also shown to act as plant defense elicitors or avirulence (*avr*) factors when detected by a corresponding pathogen recognition (R) protein in the host (Jones & Dangl, 2006). *P. syringae* has evolved a functionally redundant repertoire of effectors, which allows pathogen populations to lose/modify expendable *avr* elicitors, with minimal impact on overall virulence (Arnold & Jackson, 2011). It is believed that as pathogen lineages specialise, they fine-tune their effector repertoires to maximize virulence and avoid detection. Host range becomes restricted because the pathogen may lose effectors important for disease on other hosts or gain effectors detected by other plant species (Schulze-Lefert & Panstruga, 2011). Many genomics studies have therefore focused on identifying patterns that link effector complements with particular diseases (Baltrus *et al.* 2011, 2012; O'Brien *et al.* 2012).

Much of the understanding of *P. syringae* – plant interactions has been achieved using herbaceous plant models. Woody, perennial pathosystems provide a greater challenge (Lamichhane *et al.*, 2014). Population genomics of *P.s* pv. *actinidiae*, the causal agent of kiwifruit canker, revealed that three pathogen clades, with distinct effector gene sets, have arisen during kiwifruit cultivation (McCann *et al.*, 2013, 2017). A study of the olive pathogen *P.s* pv. *savastanoi* revealed that the *hopBL* effector family is over-represented in wood-infecting pathovars (Matas *et al.*, 2014). Apart from effectors, genes involved in the metabolism of aromatic compounds, phytohormone production and tolerance to reactive oxygen species have been implicated in virulence on olive (Buonaurio *et al.*, 2015). Bartoli *et al.* (2015a) found that the degradation of the aromatic compound catechol was important for symptom development of *P.s* pv. *actinidiae* on kiwifruit. Green *et al.* (2010), identified differences in sucrose metabolism that may dictate the tissue specificity of *P.s* pv. *aesculi* strains that infect horse chestnut. Nowell *et al.* (2016) also identified genes significantly associated with the woody niche. They found candidate effectors, xylose degradation and the α-ketoadipate pathway were associated with this niche.

This study used genomics to examine the evolution of strains that cause bacterial canker on sweet and wild cherry (both *Prunus avium*). Clades of *P. syringae* that constitute the main causal agents of bacterial canker include *P.s* pv. *morsprunorum* (*Psm*) race 1 and race 2 and a *P.s* pv. *syringae* (*Pss*) (Bultreys & Kaluzna, 2010). In addition, *P.s* pv. *avii* causes bacterial canker of wild cherry (Ménard *et al.*, 2003). Recently proposed revisions to species names placed *Psm* R1 in *P. amygdali* and *Psm* R2 in *P. avellanae* (Bull *et al.*, 2010). As they are part of the *P. syringae* species complex they will be referred to as *Psm* in this study. The cherry-pathogenic clades of *P. syringae* are reported to exhibit differences in virulence, host range and lifestyle (Scortichini 2010; Crosse & Garrett 1966), making the *P. syringae*-cherry pathosystem an intriguing opportunity to study convergent specialisation. The genomic analysis has been coupled with robust pathogenicity testing (Hulin *et al.*, 2018) and functional analysis of potential avirulence (*avr*) genes. This study provides a proof-of-concept that genomics-based predictions can be used to identify candidate genes involved in disease and will likely become the major tool in disease monitoring, diagnostics and host range prediction.

Materials and methods

Bacteria, plants and pathogenicity tests

Methods used for bacterial culture and sources of plants were as described in Hulin *et al.* (2018) and are detailed in supplementary methods. Bacterial strains are listed in Table 1. *Escherichia coli* was plated onto Lysogeny Broth Agar (LBA) and grown overnight at 37 °C. Antibiotic concentrations (µg/ml): Kanamycin 50, Gentamycin 10, Spectinomycin 100, Nitrofurantoin 100. X-gal was used at a concentration of 80µg/ml. Tables S1-S3 list the *P. syringae* mutants, plasmids and primers used in this study.

Pathogenicity tests, performed on detached cherry leaves and analysed as in Hulin *et al.* (2018) are described in the supplementary methods. All ANOVA tables are presented in Tables S17-25.

Genome sequencing, assembly and annotation

Genome sequencing using Illumina and genome assembly were performed as in Hulin *et al.* (2018). For long-read sequencing, PacBio (Pacific Biosystems) and MinION (Oxford Nanopore) were used. High molecular weight DNA was extracted using a CTAB method (Feil *et al.*, 2012). For the PacBio sequencing of *Psm* R1-5244, R2-leaf and syr9097, DNA samples were sent to the Earlham Institute (Norwich) for PacBio RSII sequencing.

For MinION sequencing of *Psm* R1-5300, the DNA library was prepared using the RAD001 rapid-prep kit and run on the Oxford Nanopore MinION, flowcell version R9.5 followed by basecalling using Metrichor. MinION reads were extracted from Fast5 files using Poretools (Loman & Quinlan, 2014). The sequencing reads for both long-read technologies were trimmed and assembled using Canu (Berlin *et al.*, 2015) and Circlator was used to circularise contigs (Hunt *et al.*, 2015). The assemblies were polished using error-corrected Illumina reads with bowtie2, samtools and Pilon 1.17 (Li *et al.*, 2009; Langmead & Salzberg, 2013; Walker *et al.*, 2014).

Plasmid profiling was performed using an alkaline-lysis method (Moulton *et al.*, 1993) and viewed by gel electrophoresis as in Neale *et al.* (2013). Genomes were submitted to Genbank and accession numbers are listed in Table 1.

Orthology analysis

OrthoMCL (Li *et al.*, 2003) was used to identify orthologous genes. 108 genomes, including those sequenced and those downloaded from NCBI were re-annotated using RAST (Aziz *et al.*, 2008) to ensure similar annotation quality. For this reason, the Illumina short-read assemblies of the four long-read sequenced genomes (R1-5244, R1-5300, R2-leaf and syr9097) were used in orthology analysis. OrthoMCL was run with default settings and a 50 residue cut-off length.

Phylogenetic and genomic analysis of *P. syringae*

Single-copy genes present in all genomes were aligned using ClustalW (Larkin *et al.*, 2007) and trimmed using Gblocks (Castresana, 2000). Gene alignments were concatenated using Geneious (Kearse *et al.*, 2012). The program jmodeltest 2.1.10 (Posada, 2008) determined the correct evolutionary model for each gene. RAxML-AVX v8.1.15 (Stamatakis, 2014) was used in partitioned mode to build the maximum likelihood phylogeny, with a GTR gamma model and 100 non-parametric bootstrap replicates. To detect core genes that may have undergone recombination, the program GENECONV (Sawyer, 1989) was used as in Yu *et al.* (2016). Whole genome alignments were performed using progressiveMauve (Darling *et al.*, 2010).

Virulence and mobility gene identification

All T3E encoding sequences were downloaded from *pseudomonas-syringae*.org, including the recent classification of HopF effectors into four alleles (Lo *et al.*, 2016). tBLASTn (Altschul *et al.*, 1990), was used to search for homologues with a score of ≥70% identity and ≥40% query length to at least one sequence in each effector family. Nucleotide sequences were manually examined for frameshifts or truncations. Disrupted genes were classed as pseudogenes. A heatmap of effector presence was generated using heatmap.2 in gplots (Warnes *et al.*, 2016). Interproscan (Quevillon *et al.*, 2005) identified protein domains and Illustrator for Biological Sequences (IBS) was used for visualisation (Liu *et al.*, 2015). Genomic regions containing effectors were aligned using MAFFT (Katoh *et al.*, 2002).

A similar analysis was performed for phytotoxin biosynthesis, wood-degradation, ice nucleation and plasmid-associated genes. Protein sequences were obtained from NCBI (Table S4) and blasted against the genome sequence as above. Prophage identification was performed using PHASTER (Arndt *et al.*, 2016).

194

195 **Gain and loss analysis**

196 GLOOME (Gain Loss Mapping Engine) was used to plot the gain and loss of genes on the
197 core genome phylogeny (Cohen *et al.*, 2010). Effector genes were considered present even if
198 predicted to be pseudogenes, as these can still be gained and lost. The optimisation level was
199 set to "very high", a mixture model allowing variable gain and loss distributions was used
200 and the distribution type was GENERAL_GAMMA_PLUS_INV. Highly probable events
201 (probability ≥0.80) on the branches leading to cherry-pathogenic strains were extracted.

202 **BayesTraits analysis**

203 BayesTraits was used to correlate T3E gene evolution with pathogenicity (Pagel, 2004). A
204 binary matrix was created of effector family presence and pathogenicity of each strain. The
205 effector matrix was collapsed into effector families as the different alleles were predicted to
206 perform similar biological functions *in planta* (Cunnac *et al.*, 2011). Putative pseudogenes
207 were considered absent as they may be non-functional. A full description of the BayesTraits
208 methodology is described in the supplementary methods.

209

210 **Horizontal gene transfer analysis**

211 For each effector family, best hit nucleotide sequences were aligned using clustalW (Larkin
212 *et al.*, 2007). RAxML was used to build a phylogenetic tree with a GTR model of evolution
213 and 1000 bootstrap replicates. Incongruence with the core genome tree was examined
214 visually. To further assess horizontal transfer, a species-gene tree reconciliation method
215 RANGER-DTL (Bansal *et al.*, 2012) was used, as in Bruns *et al.* (2017). Full details of this
216 are described in the supplementary methods.

217

218 **Identification of genomic islands**

219 Genomic islands (GIs) were identified in the PacBio-sequenced strains using IslandViewer3
220 (Dhillon *et al.*, 2015). Islands were manually delimited as in McCann *et al.* (2013). BLASTn
221 was utilised to determine if these GIs were present in other *P. syringae* strains. As most GIs
222 exceeded 10kb, the islands were split into 0.5kb sections prior to analysis. An island was
223 concluded to be fully present if all sections produced hits with a query length >30%. To
224 validate this approach, the Illumina-sequenced genome assemblies of the PacBio-sequenced
225 strains were searched for their own islands.

226

General DNA manipulations and bacterial transformations

Cloning and other molecular biology techniques including ectopic expression of potential *avr* genes were as described in earlier works (Staskawicz *et al.*, 1984; Arnold *et al.*, 2001; Kvitko & Collmer, 2011). Details are provided in the supplementary methods.

Results

Genome assembly and sequencing statistics

Genome information gathered in this study enabled a comprehensive analysis and meaningful comparisons to investigate the evolution of pathogenicity amongst *P. syringae* pathogens of cherry. Eighteen *P. syringae* strains isolated from cherry and plum were phenotyped for pathogenicity and genome sequenced in a previous study (Hulin *et al.*, 2018). To increase this sample, nine strains isolated from wild cherry and five additional non-*Prunus* out-groups were genome-sequenced using the Illumina MiSeq. The genomes of eight cherry strains sequenced elsewhere were also downloaded from NCBI (Baltrus *et al.*, 2011; Nowell *et al.*, 2016).

Information on the origin and pathogenicity of each strain is summarised in Table 1. Twenty-eight were considered pathogenic to cherry including all *Pss* isolated from cherry and plum. In contrast, three *Psm* race 1 strains from plum (R1-5300, R1-9326 and R1-9629) and one from cherry strain (R1-9657) failed to induce canker on cherry following tree inoculations; and three strains of unknown taxonomy isolated from plum and cherry (*Ps*-9643, Ps-7928C and Ps-7969) were non-pathogenic (references in Table 1). The cherry pathogens are referred to as their described pathovar names throughout this study. To simplify figures, the first few letters of the pathovar name were used. "*Pss*" becomes "*syr*", as otherwise *Pss* could refer to other pathovars beginning with "s", e.g. *savastanoi*.

All cherry/plum isolated strains included in this study were sequenced using Illumina MiSeq. Three representative strains (R1-5244, R2-leaf and syr9097) were sequenced using PacBio and the non-pathogenic *Psm* R1 strain R1-5300 was sequenced using Oxford Nanopore, to obtain more complete genomes. Table 2 summarises the genome assembly statistics for all strains sequenced in this study and Hulin *et al.* (2018). Illumina genomes assembled into 23-352 contigs, whilst the long-read sequenced genomes assembled into 1-6 contigs. The numbers of plasmids in each strain was determined by plasmid profiling (Fig. S1). *Psm* R1

and R2 strains possessed between 2-6 plasmids, *P.s.* pv. *avii* 5271 possessed six plasmids, whereas, apart from three strains (syr5275, syr7928A, syr9644) with one plasmid each, most cherry-pathogenic strains of *Pss* did not possess plasmids. The strain syr9097 that was PacBio-sequenced lacked plasmids. The long-read sequenced genomes all assembled into the correct number of contigs corresponding to chromosome and plasmids, apart from R1-5300. The chromosome of this strain was separated into two contigs (tig0 and tig75) based on a whole genome alignment with *Psm* R1 strain R1-5244 (Fig. S2).

The *Psm* R1 (R1-5244, R1-5300) and *Psm* R2 (R2-leaf) long-read assemblies contained putatively complete plasmid contigs. These were confirmed to contain plasmid-associated genes (Tables S5-S7). All three strains (R1-5244, R1-5300 and R2-leaf) possessed plasmids with *repA* homologues, indicating they may belong to common plasmid family pPT23A (Zhao *et al.*, 2005). Several plasmids also contained conjugational machinery so may be conjugative.

Core-genome phylogenetic analysis

To examine the relatedness of strains, an analysis of core genes was carried out. 108 genomes of strains from the well studied phylogroups 1-3 isolated from both plants and aquatic environments were selected. A maximum likelihood phylogeny based on 1035 concatenated core genes was constructed using RAxML (Fig. S3). There was low support for certain P2 and P3 clades based on bootstrap analysis. To determine if particular taxa were causing low support, the analysis was systematically repeated for the two phylogroups, with non-cherry strains removed. Support and tree likelihood values were compared (Table S8). Within P3, the removal of *P.s* pv. *eriobotryae* or *P.s* pv. *daphniphylli* improved support, whilst the removal of *P.s* pv. *syringae* 1212 improved support values in P2 (Fig. S4 and S5). The global analysis was then repeated with these taxa removed (Fig. S6-S9). The final phylogeny (Fig. 1), with the highest mean branch support (92.8%) lacked *P.s.* pv. *eriobotryae*. The phylogeny, built using a 611,888bp alignment, contained 102 taxa due to the removal of identical strains (dendro4219, syr9630, R1-9629, R1-9326 and R1-5269). Most support values exceeded 70%, with good support for branches leading to cherry-pathogenic clades.

One explanation for the low support within P2 and P3 was that these clades have undergone core genome recombination. The program GENECONV (Sawyer, 1989) showed that 140 genes had putatively recombined (127,288bp total length, 20.8% of the alignment). Table S9

lists the number of recombination events per phylogroup. It was observed that the most frequent core gene recombination occurred in P3 (73 genes affected), followed by 31 genes in P2 and only 13 in P1.

Cherry pathogens were found in all three phylogroups. The two *Psm* races (R1 in P3, R2 in P1) and *P.s* pv. *avii* (P1) formed monophyletic clades. Within *Psm* R1, cherry pathogenic strains formed a distinct clade from previously classified non-pathogenic strains (Hulin *et al.*, 2018). This indicated there has been divergence in their core genomes. By contrast, *Prunus*-infecting strains of *Pss* were found across P2, interspersed with strains isolated from other plants and aquatic environments. To ensure that genomic comparisons between P2 strains were based on differential pathogenicity, several closely related non-*Prunus* strains were pathogenicity tested on detached cherry leaves (Fig. S10). *In planta* bacterial populations of non-*Prunus* strains were reduced compared to two cherry and plum *Pss* strains, indicating that host specificity may exist in P2.

Search for virulence factors

The *hrp* pathogenicity island

All sequenced strains were confirmed to contain the *hrp* pathogenicity island required for conventional Type III secretion. Core effectors genes from the conserved effector locus (CEL, Alfano *et al.*, 2000) such as *avrE1*, *hopM1* and *hopAA1*, were also present (Fig. S11), However, *hopAA1* was truncated in both *Psm* R1 and R2 due to inversion events. The *hopAA1* gene was truncated in *Psm* R2, whilst in *Psm* R1 both *hopAA1* and *hopM1* were truncated (Fig. S12).

Type III effectors and other virulence genes

All 102 genomes used in the phylogenetic analysis were scanned for known T3Es and non-T3 virulence factors. A heatmap of virulence factor presence, absence and pseudogenisation was constructed (Fig. 2). In terms of T3Es, there was variation both between and within the different cherry-pathogenic clades. Notably, *Psm* R1 which contained pathogenic and non-pathogenic strains on cherry showed clear differentiation in effector repertoire (Table S10). *Psm* R1, R2 and *P.s* pv. *avii* possessed 24-34 effector genes, whereas *Pss* strains possessed 9-15. This reduced effector repertoire of *Pss* was representative of P2 strains as noted by

Dudnik & Dudler (2014). Table 3 lists the effectors in each long-read genome assembly in order of appearance.

Non-T3 virulence factors were also identified. All pathogenic *Psm* R1 strains possessed the coronatine biosynthesis clusters, which were plasmid-borne in *Psm* R1-5244. All cherry-pathogenic *Pss* strains possessed at least one biosynthesis gene cluster for the toxins syringomycin, syringolin and syringopeptin, with several strains possessing all three. Strains within clade P2b possessed the biosynthesis genes for mangotoxin. The non-pathogenic cherry P2b strains Ps7928C and Ps7969 lacked all toxin biosynthesis clusters.

A cluster of genes named WHOP (woody hosts and *Pseudomonas*) thought to be involved in aromatic compound (lignin) degradation (Caballo-Ponce *et al.*, 2016) was present in *Psm* R1 and R2, whilst *P.s* pv. *avii* and most *Pss* strains contained no WHOP homologues. Two cherry P2d strains (syr2339 and syr7924) did however possess the catechol *catBCA* cluster. Finally, the genomes were searched for the ice nucleation gene cluster. Members of *Psm* R1, *Pss* and *P.s* pv. *avii* strains all possessed genes involved in ice nucleation (Fig. 2). Whilst Psm R2 lacked the complete set of genes for ice nucleation.

Associating T3E evolution with host specificity

T3E evolution was statistically correlated with cherry pathogenicity, using the programs BayesTraits and GLOOME (Pagel, 2004; Cohen *et al.*, 2010). BayesTraits takes a binary matrix of two traits and a phylogeny and determines if changes in the two characters (effector gene and pathogenicity) have evolved independently or dependently. Fig. 3a shows the likelihood ratio of cherry pathogenicity being correlated with each effector family's evolution, with significantly associated effectors highlighted.

BayesTraits analysis using the core genome phylogeny predicted the evolution of six T3E families was linked to cherry pathogenicity. These were *hopBF*, *hopAB*, *hopH*, *hopAR*, *avrPto* and *hopBB*. To account for any phylogenetic uncertainty, the program was also run on the full set of 100 bootstrapped trees generated by RAxML. The evolution of T3Es *hopBF*, *hopAR* and *hopAB* was always associated with pathogenicity for all 100 trees, indicating

strong association. Whilst, the T3E genes *avrPto*, *hopBB* and *hopH* were only significantly correlated for 88%, 77% and 62% of trees respectively (Fig. S13). To determine how these genes had been gained or lost across the phylogeny, the program GLOOME was used (Cohen *et al.*, 2010). Fig. 3b illustrates the predicted gain and loss of these T3Es on the branches leading to cherry pathogenic clades (with gene presence/absence profiles shown in Fig. 3c). Those putatively associated with pathogenicity (high probability of gain in cherry-pathogenic clades) included *hopAR1*, *hopBB1*, *hopBF1* and *hopH1*. The T3Es *hopAB1* and *avrPto1* were found to be lost from cherry pathogenic *Psm* R1, whilst the *hopAB1* and *hopAB3* alleles were pseudogenised in *Psm* R2 and *P.s* pv. *avii* (Fig. 3c). All effector gain and loss events are presented in Fig. S14 and Table S11. Fig. S15 shows the phylogeny with branch labels used in GLOOME.

GLOOME predicted that key effectors have been gained in multiple clades. The *hopAR1* gene has been gained in *Psm* R1, *Psm* R2, *Pss* and *P.s* pv. *avii*. The T3E *hopBB1* was present in the majority of strains within *Psm* R1, R2 and *P.s* pv. *avii* but was absent in *Pss* strains. It showed high probability of gain on branches leading to both *Psm* R2 and *P.s* pv. *avii*. However, GLOOME predicted loss in two *Psm* R1 strains indicating it has experienced dynamic evolution in cherry pathogens. The *hopBB1* effector is closely related to members of the *hopF* family and *avrRpm2* (Lo *et al.*, 2016). In addition to the significant acquisition of *hopBB1* homologues, the *hopF* family was expanded in cherry pathogens. Pathogenic strains in *Psm* R1 and R2 all possessed two *hopF* alleles each (*hopF3* and *hopF4*/*hopF2* and *hopF4*, see Fig. 2). *P.s* pv. *avii* did not possess any *hopF* homologues, but had gained *hopBB1*. By contrast, *Pss* strains lacked all *hopF* members.

Origins of key effectors in cherry pathogens

To understand the origins of key effectors, gene phylogenies were produced. Incongruence with the core-genome phylogeny indicated that effector sequences had likely experienced HGT between the pathogenic clades, as their sequences clustered together. There has been possible effector exchange between *Psm* R1, R2 and *P.s* pv. *avii*. To predict precisely where transfers had occurred on the phylogeny, the program RANGER-DTL was utilised (Bansal *et al.*, 2012). Table 4 reports T3Es that exhibited evidence of HGT between cherry pathogens (gene trees are presented in Fig. S16-S17). Full transfer events are listed in Table S12 and Fig. S18 shows the phylogeny with branch labels used in RANGER-DTL. The BayesTraits correlated T3Es *hopBB* and *hopBF* both showed evidence of HGT. Fig. 4a shows examples

of T3Es putatively undergoing HGT between cherry pathogenic clades highlighted in red. Alignments of the flanking regions (Fig. 4b) showed homology between the cherry pathogens and included mobile elements likely involved in recombination events. For example, the regions surrounding *Psm* R1 and R2 *avrD1* sequences were identical (Fig. 4b), indicating that this effector has probably been gained on the same mobile region in both clades. Putatively transferred effectors were mostly plasmid-encoded in the long-read genomes (Table 3). In R1-5244 several of these genes were encoded on one plasmid (Contig 3), whilst in R2-leaf they were found on two plasmids (Contig 6 and 8).

The pathogenicity-associated T3E gene *hopAR1* was present in 23/28 cherry pathogens and showed probable gain in pathogenic clades. Phylogenetic analysis of this T3E (Fig. 5a) showed that the sequences for the different cherry pathogenic clades did not cluster with each other, indicating convergent acquisition. Prophage-identification (Table S13) did however reveal that this T3E is predicted to have been gained in *Psm* R1 and R2 within different phage sequences, whilst in *Pss* it is on a genomic island (Fig. 5b), so has been acquired via distinct mechanisms. The *Psm* R1 phage is 51.5kb, described as intact and contains both *hopAR1* and a truncated version of *hopBK1*. The *Psm* R2 phage sequence was 37.1kb and was described as 'incomplete', indicating it did not have all the components of an active prophage. Further analysis of this region in *Psm* R2 and P2 strains revealed a shared adjacent tRNA-Thr gene (Fig. 5c,d). Within P2, although cherry *Pss* strains lacked the phage, several strains isolated from bean (syr2675, syr2676 and syr2682) possessed the *hopAR1* gene within a phage homologous to that in *Psm* R2. The syr2675 *hopAR1* sequence was also the most closely related homologue of *Psm* R2 *hopAR1* (Fig. 5a). This novel evidence suggests that this effector gene may have been transferred via phage between phylogroups.

Many T3Es are mobilised between bacteria on genomic islands (GI). GIs were identified for the three PacBio-sequenced strains of *Psm* R1, *Psm* R2 and *Pss* (Tables S14-S16). R1-5244 GIs contained the coronatine biosynthesis cluster and six T3Es. In R2-leaf, eight T3E genes were located on GIs, whilst in syr9097 three T3Es were found on genomic islands.

These GIs were then searched for in other *P. syringae* genomes to identify potential sources of transfer and Fig. 6a shows heatmaps of GI presence. The *Psm* R1 GIs included several found only in pathogenic *Psm* R1 strains differentiating them from the non-pathogens. These included the coronatine biosynthesis cluster (GI1), *hopF3* (GI6) and *hopAT1* (GI14). Most

Psm R1 GIs produced hits across *P. syringae*, particularly in P1 and P3. *Psm* R2 GIs were most commonly found in P1. Several were shared with other cherry-pathogenic clades, including those containing *hopAF1* (GI36), *hopAT1* (GI3) and *hopD1* (GI6). Finally, although most islands identified in syr9097 were commonly found across the species complex, those containing T3Es (GI30, GI23 and GI26) appeared to be P2-specific, indicating that cherry-pathogenic strains likely gained these islands from other members of P2.

Functional analysis of potential *avr* genes

To validate the predictive power of this analysis, cloning was used to identify avirulence factors active in cherry. The effector genes *avrPto* and *hopAB* were absent from cherry pathogens and their evolution was theoretically linked to pathogenicity. Several other candidate avirulence effectors were identified, that were absent from cherry pathogens, but present in close out-groups (Fig. 2). Avirulence-gene identification focused on *Psm* R1 as any T3E variation within the clade may be due to differences in host specificity rather than phylogenetic distance. Potential avirulence T3E genes included *avrA1*, *avrPto1*, *hopAA1*, *hopAB1*, *hopAO2* and *hopG1*, which had full-length homologues in non-pathogenic *Psm* R1 strains, but were absent from or truncated in pathogens. These genes were cloned from R1-5300 (except *hopAO2*, which was cloned from R1-9657).

The effector *avrRps4* was also cloned from *P.s* pv. *avellanae* (*Psv*) BPIC631 a close relative of *Psm* R2. This effector was absent from most cherry-pathogenic strains. Several pathogens possessed the full-length gene (R2-leaf, R2-9095 and *P.s* pv. *avii*), but lacked the KRVY domain that functions *in planta* (Fig. S19) (Sohn *et al.*, 2009). The *hopAW1* gene was cloned from *Pph*1448A as this T3E has undergone two independent mutations in *Pss* strains, disrupting the beginning of the gene (Fig. S20). Finally, *hopC1* was cloned from the *Aquilegia vulgaris* pathogen RMA1 which is basal to the *Psm* R2 clade, as it is absent from all cherry-pathogenic strains.

Nine effectors were cloned into the expression vector pBBR1MCS-5 and conjugated into three pathogenic strains (R1-5244, R2-leaf and syr9644). Knock-out strains for the T3SS gene *hrpA* were obtained for R1-5244 and R2-leaf to act as non-pathogenic controls that could not secrete T3Es and failed to cause the HR on tobacco (Fig. S21).

Bacterial population counts were conducted in cherry leaves. The transconjugants expressing HopAB1 or HopC1 failed to multiply to the same levels as the pathogenic empty vector (EV) controls or produce disease lesions. The expression of AvrA1, AvrRps4, and HopAW1 also caused significant reductions in population growth, but this reduction was not consistently seen across all three pathogenic strains (Fig. 7a). As the addition of the *hopAB1* gene reduced pathogenicity, the *hopAB2* and *hopAB3* genes were also cloned from *Psv*BPIC631 and RMA1, and were also found to reduce pathogen multiplication (Fig. 7b).

To further investigate the induction of the HR by the HopAB family and HopC1, inoculations were performed at high concentrations ($2x10^8$ CFU/ml) as described in Hulin *et al.* (2018). In *Psm* R1 and R2, the addition of these T3Es led to more rapid tissue collapse than observed in EV controls, indicative of HR induction (Fig. 7c,d); HopC1 and HopAB1 were particularly effective. With *Pss*, however, EV transconjugants themselves caused rapid tissue collapse, making it impossible to recognise an induced HR as symptom development was not significantly different.

The *hopAB1* gene is found in a mobile-element rich ~40kb region in the non-pathogenic *Psm* R1-5300, missing from the pathogen *Psm* R1-5244 (Fig. 7d). Meanwhile, *Psm* R2 and *P.s* pv. *avii* possessed putatively pseudogenised *hopAB3* alleles (Fig. 7e) and *P.s* pv. *avii* possessed a truncated *hopAB1* gene (Fig. S22). *hopAB3* is truncated in *Psm* R2 due to a 2bp insertion (GG at position 1404bp) leading to a premature stop codon, whilst in *P.s* pv. *avii* a 218bp deletion has disrupted the C-terminus. If expressed, the E3-ubiquitin ligase is completely absent from the *Psm* R2 protein and disrupted in *P.s* pv. *avii* (Fig. 7f). Both HopAB3 alleles were also divergent enough that the Pto-interacting domain (PID) was not identified by Interproscan. To determine if the truncated *Psm* R2 HopAB3 allele induced any resistance response in cherry leaves, the gene was expressed in *Psm* R1-5244 and population growth measured. The addition of this gene did not lead to a significant reduction in growth compared to the EV control, unlike other *hopAB* alleles (Fig. 7g) and the transconjugant was still able to induce disease symptoms 10 dpi (Fig. 7h).

Discussion

Core genome phylogenetics

Phylogenetic analysis confirmed that cherry pathogenicity has evolved multiple times within *P. syringae*. *Psm* R1, R2 and *P.s* pv. *avii* each formed distinct monophyletic clades, whereas cherry-pathogenic *Pss* strains were distributed across the P2 clade thus indicating that cherry pathogenicity has either evolved multiple times within P2 or that this clade is not highly specialised. To confirm this genomic prediction of pathogenicity, several additional P2 strains isolated from bean, pea and lilac were tested for pathogenicity in cherry. They each produced lower population levels in cherry leaves than cherry pathogens, suggesting that host adaptation has occurred (Fig. S10). Many P2 strains have previously been named *Pss* on the basis of lilac pathogenicity, despite being pathogenic to other plant species (Young, 1991). A new naming system within this phylogroup would therefore be desirable.

Search for candidate effectors involved in cherry pathogenicity

Gains and losses of T3Es were closely associated with pathogenicity. Virulence-associated effectors *hopAR1*, *hopBB1*, *hopH1* and *hopBF1* had been gained in multiple cherry-pathogenic clades. The *hopAR1* effector has been studied in the bean pathogen *P.s* pv. *phaseolicola* R3 (1302A), as an GI-located *avr* gene (*avrPphB*) whose protein is detected by the corresponding R3 resistance protein *in planta* (Pitman *et al.*, 2005; Neale *et al.*, 2016). HopAR1 also acts as a virulence factor as a cysteine protease which targets receptor-like kinases to interfere with plant PAMP-triggered immunity (PTI) responses (Zhang *et al.*, 2010). This effector could play a similar role in PTI suppression in cherry.

HopBB1 and other members the HopF family were abundant in cherry pathogens. All HopF members share an N-terminus and myristoylation sites for plant cell membrane localisation (Lo *et al.*, 2016) and interfere with PTI and Effector-triggered immunity (ETI) in model plants (Wang *et al.*, 2010; Wu *et al.*, 2011; Hurley *et al.* 2014). The presence of multiple *hopF* homologues in cherry pathogens and specific gain of *hopBB1* suggested the importance of their function. In comparison, HopH1 and HopBF1 are under studied. HopH1 is a protease, homologous to the *Ralstonia solanacearum* Rip36 protein (Nahar *et al.*, 2014). This T3E gene was found on GI37 in *Psm* R2-leaf and was within 3kb of *hopF4* (Fig. S23), indicating that these two T3Es may have been gained together. HopBF1 was first discovered in *P.s* pvs *aptata* and *oryzae* (Baltrus *et al.*, 2011) but its role *in planta* is undetermined. This study therefore provided candidate T3Es important for cherry pathogenicity which could be the focus of future functional studies.

Phytotoxin biosynthesis gene clusters were also identified. Coronatine has been gained on a plasmid in pathogenic *Psm* R1 and could be one of the factors that differentiate pathogens from non-pathogens in this clade. Coronatine functions in virulence by down-regulating salicylic acid defence signalling (Grant & Jones, 2009). Necrosis-inducing lipodepsipeptide toxins were common in P2. All cherry-pathogenic *Pss* strains possessed at least one biosynthesis cluster. The ability of *Pss* strains to cause necrosis on cherry fruits has been linked to toxins (Scholz-Schroeder *et al.*, 2001). Interestingly, two non-pathogenic P2b cherry strains lacked all phytotoxins, a deficiency that could contribute to their lack of pathogenicity.

All cherry-pathogenic *Pss* strains had reduced effector repertoires. This observation supports the hypothesis that a phenotypic trade-off exists, with strains retaining few T3Es, whilst relying more on phytotoxins for pathogenicity (Hockett *et al.*, 2014). If this pathogenic strategy has evolved in the P2 clade, this raises the question as to how it affects host specificity and virulence. P2 strains often infect more than one host species (Rezaei & Taghavi, 2014). These strains probably possess fewer ETI-inducing avirulence factors that restrict effector-rich strains to particular hosts, so may be more successful generalists. The reduction in T3E repertoire could however be limiting as strains may be less capable of long-term disease suppression required at the start of a hemi-biotrophic interaction.

Most cherry-pathogenic clades possessed genes involved in aromatic compound degradation, shown to be important in virulence on olive (Caballo-Ponce *et al.*, 2016) and ice nucleation genes that stimulate frost damage (Lamichhane *et al.*, 2014). The fact that not all cherry-pathogenic clades possessed these genes suggests they are not crucial for bacterial canker, however they could contribute to niche persistence. For example, Crosse and Garrett (1966), observed that *Psm* R1 survived in cankers for longer than *Pss*. Increased persistence could be linked to genes involved in woody-tissue adaptation.

HGT has been important in the acquisition of key effectors

HGT is a key mechanism for effector shuffling within *P. syringae* (Arnold & Jackson, 2011). Pathogenicity-associated T3Es *hopBB1* and *hopBF1* were plasmid encoded and showed evidence of HGT between the cherry-pathogenic clades in P1 and P3. Plasmid profiling revealed that cherry pathogens in phylogroups 1 and 3 possessed native plasmids, some of

562 which were putatively conjugative, indicating the importance of plasmids in gene exchange.
563 By contrast, most cherry-pathogenic *Pss* strains lacked plasmids.
564
565 The pathogenicity-associated T3E *hopAR1* was chromosomal in *Psm* R1 and R2. This gene
566 was found within distinct prophage sequences in these two clades. To our knowledge this is
567 the first reported example of a plant pathogen T3E located within a prophage sequence.
568 Interestingly, the *Psm* R2 *hopAR1* gene homologue was most similar to *hopAR1* from a P2
569 bean strain syr2675, which is a close relative of cherry *Pss*. This strain possessed the same
570 phage as *Psm* R2, indicating that horizontal gene transfer of this T3E between phylogroups
571 may have been phage-mediated. The striking example of convergent acquisition of *hopAR1*
572 in the cherry pathogens, putatively through distinct prophages in *Psm* R1 and R2, and a GI in
573 *Pss* indicates that this T3E may have important roles in virulence. The well characterised *P.s*
574 pv. *phaseolicola* R3 homologue is not associated with a phage, but has been shown to
575 undergo dynamic evolution on a mobile genomic island *in planta* in resistant bean cultivars
576 (Neale *et al.*, 2016). It is intriguing that the same T3E may be important in a completely
577 different pathosystem.
578
579 Several T3Es in *Psm* R1, R2 and *Pss* were located on GIs. To determine the likely source of
580 GIs in cherry strains, all other *P. syringae* strains were searched for homologous sequences
581 (Fig. 6). There was evidence of *Psm* R1 and R2 islands being shared between cherry
582 pathogen clades indicative of HGT events occurring between strains occupying the same
583 ecological niche.
584
585 **Functional genomics revealed convergent loss of an avr factor**

586 Genes from the *hopAB* and *avrPto* families form a redundant effector group (REG) vital for
587 early PTI suppression in herbaceous species (Jackson *et al.*, 1999; Lin & Martin, 2005;
588 Kvitko *et al.*, 2009). Both effectors also trigger ETI by interacting with the serine-threonine
589 kinase R protein Pto in tomato (Kim *et al.*, 2002).
590
591 Across the *P. syringae* complex, the REG was common (Fig. S24), but cherry pathogens all
592 lacked full-length members of this family. The *hopAB1* gene has been lost from *Psm* R1,
593 whilst the *Psm* R2 and *P.s* pv. *avii* predicted HopAB3 proteins lacked the PID and E3-
594 ubiquitin ligase domains through contrasting mutations. *P.s* pv. *avii* also possessed a

595 truncated *hopAB1* gene (Fig. S22), lacking the PID domain. The lack of a PID in the cherry
596 pathogen HopAB proteins suggested that they could have diverged to avoid a Pto-like
597 recognition in cherry.
598
599 Full-length members of this REG were cloned into cherry pathogens to determine their role
600 *in planta*. The addition of HopAB alleles (HopAB1-3) consistently reduced population
601 growth of pathogenic strains *in planta* and triggered an HR. HopAB loss or pseudogenisation
602 in cherry pathogens may have been selected for to reduce avirulence activity. The truncated
603 version of HopAB3 in R2-leaf was found not to exhibit avirulence activity as its expression
604 did not reduce the growth of R1-5244 *in planta*. Although AvrPto is part of the same REG,
605 its expression had no effect on the ability of cherry pathogens to multiply *in planta*. The
606 absence of AvrPto in cherry pathogens is therefore unlikely to be driven by avirulence, but
607 could be due to the lack of HopAB virulence targets *in planta*. As this REG is vital for early
608 disease suppression in model strains, cherry pathogens may rely on other T3Es to fulfil this
609 role.
610
611 The variation in *hopAB1* presence in *Psm* R1 is intriguing. *Psm* R1 strains may be pathogenic
612 on both cherry and plum (Δ*hopAB1*) or just pathogenic on plum (possessed *hopAB1*) (Hulin
613 *et al.*, 2018). This suggested that the host proteins in cherry that detect the presence of
614 HopAB are not present/functioning in plum. Future studies may determine how the two host
615 immune responses diverged and could examine *hopAB* diversity across *Prunus* pathogens.
616 This study focused on *Prunus avium*, however strains isolated from additional *Prunus* spp.
617 were included, such as *P.s* pv. *cerasicola*, *P.s* pv. *morsprunorum* FTRSU7805, *P.s* pv.
618 *amygdali* and *P.s* pv. *persicae* (Table 1). All apart from *P.s* pv. *amygdali* 3205 and *P.s* pv.
619 *persicae* lacked HopAB (Fig. 2), indicating that there may be a conserved resistance
620 mechanism regulating ETI activated by this effector family in *Prunus* species.
621
622 **Linking genomics to host specialisation**
623 Cherry pathogenicity has arisen independently within *P. syringae*, with strains using both
624 shared and distinctive virulence strategies. Cherry-pathogenic clades in P1 and P3 have large
625 effector repertoires. Cherry *Pss* were found across P2. They possessed reduced T3Es and
626 several phytotoxin gene clusters. Key events in the evolution of cherry pathogenicity (Fig. 8)
627 appear to be the acquisition of virulence-associated effectors, often through horizontal gene
628 transfer, such as *hopAR1*, members of the *hopF* family such as *hopBB1*, *hopBF1* and *hopH1*.

Significantly, the loss/pseudogenisation of HopAB effectors has also occurred in multiple clades. Within P2, the different cherry-infecting *Pss* clades have slight differences in their virulence factor repertoires which may reflect their convergent host adaptation. Clades differed in T3E content, phytotoxin genes and possession of genes for catechol degradation. This study demonstrated that populations genomics can be used to examine a complex disease of a perennial plant species. A huge dataset was narrowed down to several candidate host-specificity controlling genes, two of which (*hopAB* and *hopC1*) encode proteins that had putative avirulence functions *in planta*.

Acknowledgements

We acknowledge the East Malling Trust, University of Reading and BBSRC for funding (BB/P006272/1). Library preparation for PacBio sequencing was performed at the Earlham Institute, whilst for wild cherry strains Illumina MiSeq sequencing, libraries was prepared at the Genomics Facility, University of Warwick. We thank Steve Roberts, Helen Neale, Mateo San José and David Guttman for providing bacterial strains. We thank the East Malling Farm and Glass staff for plant maintenance. The authors declare no conflict of interest.

Author contributions

MTH, JWM, RWJ and RJH conceived and designed the study as well as writing the manuscript. MTH performed bioinformatics, statistical analysis and laboratory work. JV isolated some of the strains used in this study, JV and EH selected representative strains and prepared DNA for MiSeq sequencing of nine strains and LB assembled these nine sequences. HJB performed the MinION library preparation and sequencing. ADA assisted in bioinformatics pipeline development. All authors read and reviewed the final manuscript.

References

Alfano JR, Charkowski A, Deng W, Badel J, Petnicki-Ocwieja T, van Dijk K, Collmer A. 2000. The *Pseudomonas syringae* Hrp pathogenicity island has a tripartite mosaic structure composed of a cluster of type III secretion genes bounded by exchangeable effector and conserved effector loci that contribute to parasitic fitness and pathogenicity in pl. *Proceedings of the National Academy of Sciences of the United States of America* **97**: 4856–4861.

Almeida NF, Yan S, Lindeberg M, Studholme DJ, Schneider DJ, Condon B, Liu H, Viana CJ, Warren A, Evans C, *et al.* 2009. A draft genome sequence of *Pseudomonas syringae* pv. *tomato* T1 reveals a type III effector repertoire significantly divergent from that of *Pseudomonas syringae* pv. *tomato* DC3000. *Molecular Plant-Microbe Interactions: MPMI* **22**: 52–62.

Altschul SF, Gish W, Miller W, Myers EW, Lipman DJ. 1990. Basic local alignment search tool. *Journal of molecular biology* **215**: 403–410.

Arndt D, Grant JR, Marcu A, Sajed T, Pon A, Liang Y, Wishart DS. 2016. PHASTER: A better, faster version of the PHAST phage search tool. *Nucleic acids research* **44**: W16–W21.

Arnold DL, Gibbon MJ, Jackson RW, Wood JR, Brown J, Mansfield JW, Taylor JD, Vivian A. 2001. Molecular characterization of *avrPphD*, a widely-distributed gene from *Pseudomonas syringae* pv. *phaseolicola* involved in non-host recognition by pea (*Pisum sativum*). *Physiological and Molecular Plant Pathology* **58**: 55–62.

Arnold DL, Jackson RW. 2011. Bacterial genomes: Evolution of pathogenicity. *Current opinion in plant biology* **14**: 385–391.

Aziz RK, Bartels D, Best AA, DeJongh M, Disz T, Edwards RA, Formsma K, Gerdes S, Glass EM, Kubal M, *et al.* 2008. The RAST Server: Rapid annotations using subsystems technology. *BMC genomics* **9**: 75.

Baltrus DA, Nishimura MT, Romanchuk A, Chang JH, Mukhtar MS, Cherkis K, Roach J, Grant SR, Jones CD, Dangl JL. 2011. Dynamic evolution of pathogenicity revealed by sequencing and comparative genomics of 19 *Pseudomonas syringae* isolates. *PLoS Pathogens* **7**: 22.

Baltrus DA, Nishimura MT, Dougherty KM, Biswas S, Mukhtar MS, Vicente JG, Holub EB, Dangl JL. 2012. The molecular basis of host specialization in bean pathovars of *Pseudomonas syringae*. *Molecular Plant-Microbe Interactions MPMI* **25**: 877–888.

Baltrus DA, Yourstone S, Lind A, Guilbaud C, Sands DC, Jones CD, Morris CE, Dangl JL. 2014a. Draft genome sequences of a phylogenetically diverse suite of *Pseudomonas syringae* strains from multiple source populations. *Genome Announcements* **2**: e01195-13.

Baltrus DA, Dougherty K, Beckstrom-Sternberg SM, Beckstrom-Sternberg JS, Foster JT. 2014b. Incongruence between multi-locus sequence analysis (MLSA) and whole-genome-based phylogenies: *Pseudomonas syringae* pathovar *pisi* as a cautionary tale. *Molecular plant pathology* **15**: 461–465.

Baltrus DA, McCann HC, Guttman DS. 2017. Evolution, genomics and epidemiology of *Pseudomonas syringae*. *Molecular Plant Pathology* **18**: 152-168.

Bansal MS, Alm EJ, Kellis M. 2012. Efficient algorithms for the reconciliation problem with gene duplication, horizontal transfer and loss. *Bioinformatics* **28**: 283–291.

Bartoli C, Lamichhane JR, Berge O, Guilbaud C, Varvaro L, Balestra GM, Vinatzer BA, Morris CE. 2015a. A framework to gauge the epidemic potential of plant pathogens in environmental reservoirs: The example of kiwifruit canker. *Molecular Plant Pathology* **16**: 137–149.

Bartoli C, Carrere S, Lamichhane R, Varvaro L, Morris CE. 2015b. Whole-genome sequencing of 10 *Pseudomonas syringae* strains representing different host range spectra. *Genome Announcements* **3**: 2–3.

Bender CL, Alarcón-Chaidez F, Gross DC. 1999. *Pseudomonas syringae* phytotoxins: Mode of action, regulation, and biosynthesis by peptide and polyketide synthetases. *Microbiology and molecular biology reviews : MMBR* **63**: 266–292.

Berge O, Monteil CL, Bartoli C, Chandeysson C, Guilbaud C, Sands DC, Morris CE. 2014. A user's guide to a data base of the diversity of *Pseudomonas syringae* and its application to classifying strains in this phylogenetic complex. *PLoS ONE* **9**: e105547.

Berlin K, Koren S, Chin C-S, Drake JP, Landolin JM, Phillippy AM. 2015. Assembling large genomes with single-molecule sequencing and locality-sensitive hashing. *Nature biotechnology* **33**: 623–630.

Bruns H, Crüsemann M, Letzel A-C, Alanjary M, McInerney JO, Jensen PR, Schulz S, Moore BS, Ziemert N. 2017. Function-related replacement of bacterial siderophore pathways. *The ISME Journal*: doi:10.1038/ismej.2017.

Buell CR, Joardar V, Lindeberg M, Selengut J, Paulsen IT, Gwinn ML, Dodson RJ, Deboy RT, Durkin AS, Kolonay JF, *et al.* 2003. The complete genome sequence of the *Arabidopsis* and tomato pathogen *Pseudomonas syringae* pv. *tomato* DC3000.

Proceedings of the National Academy of Sciences of the United States of America **100**: 10181–10186.

Bull CT, de Boer SH, Denny TP, Firrao G, Fischer-Le Saux M, Saddler GS, Scortichini M, Stead DE, Takikawa Y. **2010**. Comprehensive list of names of plant pathogenic bacteria, 1980-2007. *Journal of Plant Pathology* **92**: 551–592.

Bultreys A, Kaluzna M. **2010**. Bacterial cankers caused by *Pseudomonas syringae* on stone fruit species with special emphasis on the pathovars *syringae* and *morsprunorum* Race 1 and Race 2. *Journal of Plant Pathology* **92**: S1.21-S1.33.

Buonaurio R, Moretti C, da Silva DP, Cortese C, Ramos C, Venturi V. **2015**. The olive knot disease as a model to study the role of interspecies bacterial communities in plant disease. *Frontiers in plant science* **6**: 434.

Butler MI, Stockwell PA, Black MA, Day RC, Lamont IL, Poulter RTM. **2013**. *Pseudomonas syringae* pv. *actinidiae* from recent outbreaks of kiwifruit bacterial canker belong to different clones that originated in China. *PloS one* **8**: e57464.

Caballo-Ponce E, van Dillewijn P, Wittich R, Ramos C. **2016**. WHOP, a genomic region associated with woody hosts in the *Pseudomonas syringae* complex contributes to the virulence and fitness of *Pseudomonas savastanoi* pv. *savastanoi* in olive plants. *Molecular Plant-Microbe Interactions* **30**: 113–126.

Castresana J. **2000**. Selection of conserved blocks from multiple alignments for their use in phylogenetic analysis. *Molecular Biology and Evolution* **17**: 540–552.

Cohen O, Ashkenazy H, Belinky F, Huchon D, Pupko T. **2010**. GLOOME: Gain loss mapping engine. *Bioinformatics* **26**: 2914–2915.

Crosse, JE, & Garrett CME. 1966. Bacterial canker of stone-fruits. VII. Infection experiments with *Pseudomonas morsprunorum* and *Ps. syringae*. *Annals of Applied Biology* **58**: 31–41.

Cunnac S, Chakravarthy S, Kvitko BH, Russell AB, Martin GB, Collmer A. **2011**. Genetic disassembly and combinatorial reassembly identify a minimal functional repertoire of type III effectors in *Pseudomonas syringae*. *Proceedings of the National Academy of Sciences of the United States of America* **108**: 2975–2980.

Darling AE, Mau B, Perna NT. **2010**. Progressivemauve: Multiple genome alignment with gene gain, loss and rearrangement. *PLoS ONE* **5**: e11147.

Dhillon BK, Laird MR, Shay JA, Winsor GL, Lo R, Nizam F, Pereira SK, Waglechner N, McArthur AG, Langille MGI, *et al.* 2015. IslandViewer 3: More flexible,

758 interactive genomic island discovery, visualization and analysis. *Nucleic Acids Research*
759 **43**: W104–W108.
760 **Ditta G, Stanfield S, Corbin D, Helinski DR**. **1980**. Broad host range DNA cloning system
761 for gram-negative bacteria: construction of a gene bank of *Rhizobium meliloti*.
762 *Proceedings of the National Academy of Sciences of the United States of America* **77**:
763 7347–7351.
764 **Dudnik A, Dudler R**. **2014**. Genomics-based exploration of virulence determinants and host-
765 specific adaptations of *Pseudomonas syringae* strains isolated from grasses. *Pathogens*
766 **3**: 121–148.
767 **Edwards DJ, Holt KE**. **2013**. Beginner's guide to comparative bacterial genome analysis
768 using next-generation sequence data. *Microbial Informatics and Experimentation* **3**: 2.
769 **Feil H, Feil WS, Chain P, Larimer F, DiBartolo G, Copeland A, Lykidis A, Trong S,**
770 **Nolan M, Goltsman E, *et al.* 2005**. Comparison of the complete genome sequences of
771 *Pseudomonas syringae* pv. *syringae* B728a and pv. *tomato* DC3000. *Proceedings of the*
772 *National Academy of Sciences of the United States of America* **102**: 11064–11069.
773 **Feil W, Feil H, Copeland A**. **2012**. Bacterial genomic DNA isolation using CTAB. URL
774 http://1ofdmq2n8tc36m6i46scovo2e.wpengine.netdna-cdn.com/wp-
775 content/uploads/2014/02/JGI-Bacterial-DNA-isolation-CTAB-Protocol-2012.pdf
776 [accessed 28th December 2017]
777 **Gardan L, Shafik H, Belouin S, Broch R, Grimont F, Grimont P**. **1999**. DNA relatedness
778 among the pathovars of *Pseudomonas syringae* and description of *Pseudomonas tremae*
779 sp. nov. and *Pseudornonas cannabina* sp. nov. (ex Sutic and Dowson 1959).
780 *International Journal of Systematic Bacteriology* **49**: 469–478.
781 **Gardiner DM, Stiller J, Covarelli L, Lindeberg M, Shivas RG, Manners JM**. **2013**.
782 Genome sequences of *Pseudomonas* spp. isolated from cereal crops. *Genome*
783 *announcements* **1**: e00209–e00213.
784 **Gilbert V, Planchon V, Legros F, Maraite H, Bultreys A**. **2009**. Pathogenicity and
785 aggressiveness in populations of *Pseudomonas syringae* from Belgian fruit orchards.
786 *European Journal of Plant Pathology* **126**: 263–277.
787 **Grant M, Jones J**. **2009**. Hormone (dis)harmony moulds plant health and disease. *Science*
788 **324**: 750–752.
789 **Green S, Studholme DJ, Laue BE, Dorati F, Lovell H, Arnold D, Cottrell JE, Bridgett S,**
790 **Blaxter M, Huitema E, *et al.* 2010**. Comparative genome analysis provides insights

into the evolution and adaptation of *Pseudomonas syringae* pv. *aesculi* on *Aesculus hippocastanum*. *PloS one* **5**: e10224.

Guttman DS, McHardy AC, Schulze-Lefert P. **2014**. Microbial genome-enabled insights into plant–microorganism interactions. *Nature Reviews Genetics* **15**: 797–813.

Hockett KL, Nishimura MT, Karlsrud E, Dougherty K, Baltrus DA. **2014**. *Pseudomonas syringae* CC1557: A highly virulent strain with an unusually small type III effector repertoire That includes a novel effector. *Molecular Plant-Microbe Interactions: MPMI* **27**: 923–32.

Hulin MT, Mansfield JW, Brain P, Xu X, Jackson RW, Harrison RJ. **2018**. Characterisation of the pathogenicity of strains of *Pseudomonas syringae* towards cherry and plum. *Plant Pathology*. (Accepted article Dec 2017)

Hunt M, Silva N De, Otto TD, Parkhill J, Keane JA, Harris SR. **2015**. Circlator: Automated circularization of genome assemblies using long sequencing reads. *Genome Biology* **16**: 294.

Hurley B, Lee D, Mott A, Wilton M, Liu J, Liu YC, Angers S, Coaker G, Guttman DS, Desveaux D. **2014**. The *Pseudomonas syringae* type III effector HopF2 suppresses *Arabidopsis* stomatal immunity. *PLoS ONE* **9**: e114921.

Jackson RW, Athanassopoulos E, Tsiamis G, Mansfield JW, Sesma a, Arnold DL, Gibbon MJ, Murillo J, Taylor JD, Vivian a. **1999**. Identification of a pathogenicity island, which contains genes for virulence and avirulence, on a large native plasmid in the bean pathogen *Pseudomonas syringae* pathovar *phaseolicola*. *Proceedings of the National Academy of Sciences of the United States of America* **96**: 10875–80.

Joardar V, Lindeberg M, Jackson RW, Selengut J, Dodson R, Brinkac LM, Daugherty SC, Deboy R, Durkin AS, Giglio MG, *et al.* 2005. Whole-genome sequence analysis of *Pseudomonas syringae* pv. *phaseolicola* 1448A reveals divergence among pathovars in genes involved in virulence and transposition. *Journal of Bacteriology* **187**: 6488–6498.

Jones JDG, Dangl JL. **2006**. The plant immune system. *Nature* **444**: 323–329.

Kamiunten H, Nakaol T, Oshida S. **2000**. Agent of bacterial gall of cherry tree. *J. Gen. Plant Pathol.* **66**: 219–224.

Katoh K, Misawa K, Kuma K, Miyata T. **2002**. MAFFT: A novel method for rapid multiple sequence alignment based on fast Fourier transform. *Nucleic acids research* **30**: 3059–3066.

Kearse M, Moir R, Wilson A, Stones-Havas S, Cheung M, Sturrock S, Buxton S, Cooper A, Markowitz S, Duran C, *et al.* 2012. Geneious Basic: An integrated and

825 extendable desktop software platform for the organization and analysis of sequence data.
826 *Bioinformatics* **28**: 1647–1649.
827 **Kim YJ, Lin NC, Martin GB**. **2002**. Two distinct *Pseudomonas* effector proteins interact
828 with the Pto kinase and activate plant immunity. *Cell* **109**: 589–598.
829 **Kovach ME, Elzer PH, Hill DS, Robertson GT, Farris M a, Roop RM, Peterson KM**.
830 **1995**. Four new derivatives of the broad-host-range cloning vector pBBR1MCS,
831 carrying different antibiotic-resistance cassettes. *Gene* **166**: 175–6.
832 **Kvitko B, Collmer A**. **2011**. Construction of *Pseudomonas syringae* pv. *tomato* DC3000
833 mutant and polymutant strains. In: McDowell J, ed. *Plant Immunity. Methods in*
834 *Molecular Biology (Methods and Protocols)*. Humana Press, 109–128.
835 **Kvitko BH, Park DH, Velásquez AC, Wei C-F, Russell AB, Martin GB, Schneider DJ,**
836 **Collmer A**. **2009**. Deletions in the repertoire of *Pseudomonas syringae* pv. *tomato*
837 DC3000 type III secretion effector genes reveal functional overlap among effectors.
838 *PLoS pathogens* **5**: e1000388.
839 **Lamichhane JR, Varvaro L, Parisi L, Audergon J-M, Morris CE**. **2014**. Chapter Four -
840 Disease and frost damage of woody plants caused by *Pseudomonas syringae*: Seeing the
841 forest for the trees. In: Boyer J, Alexander M, Kamprath E, eds. *Advances in Agronomy*.
842 San Diego: Academic Press, 235–295.
843 **Langmead B, Salzberg S**. **2013**. Fast gapped-read alignment with Bowtie2. *Nature methods*
844 **9**: 357–359.
845 **Larkin M, Blackshields G, Brown NP, Chenna R, Mcgettigan P a., McWilliam H,**
846 **Valentin F, Wallace IM, Wilm A, Lopez R, *et al.* 2007**. Clustal W and Clustal X
847 version 2.0. *Bioinformatics* **23**: 2947–2948.
848 **Leong S, Ditta G, Helinshi D**. **1982**. Heme biosynthesis in *Rhizobium*: identification of a
849 cloned gene coding for deltaaminolevulinic acid synthetase from *Rhizobium meliloti*.
850 *Journal of Biological Chemistry* **257**: 8724–8730.
851 **Li H, Handsaker B, Wysoker A, Fennell T, Ruan J, Homer N, Marth G, Abecasis G,**
852 **Durbin R**. **2009**. The Sequence Alignment/Map format and SAMtools. *Bioinformatics*
853 **25**: 2078–2079.
854 **Li L, Stoeckert CJJ, Roos DS**. **2003**. OrthoMCL: Identification of ortholog groups for
855 eukaryotic genomes. *Genome Research* **13**: 2178–2189.
856 **Lin NC, Martin GB**. **2005**. An *avrPto*/*avrPtoB* mutant of *Pseudomonas syringae* pv. *tomato*
857 DC3000 does not elicit Pto-mediated resistance and is less virulent on tomato.
858 *Molecular Plant-Microbe Interactions MPMI* **18**: 43–51.

Lindgren PB. **1997**. The role of *hrp* genes during plant-bacterial interactions. *Annual review of phytopathology* **35**: 129–52.

Liu H, Qiu H, Zhao W, Cui Z, Ibrahim M, Jin G, Li B, Zhu B, Xie GL. **2012**. Genome sequence of the plant pathogen *Pseudomonas syringae* pv. panici LMG 2367. *Journal of Bacteriology* **194**: 5693–5694.

Liu W, Xie Y, Ma J, Luo X, Nie P, Zuo Z, Lahrmann U, Zhao Q, Zheng Y, Zhao Y, *et al.* 2015. IBS: An illustrator for the presentation and visualization of biological sequences. *Bioinformatics* **31**: 3359–3361.

Lo T, Koulena N, Seto D, Guttman DS, Desveaux D. **2016**. The HopF family of *Pseudomonas syringae* type III secreted effectors. *Molecular Plant Pathology* **18**: 1–12.

Loman NJ, Quinlan AR. **2014**. Poretools: A toolkit for analyzing nanopore sequence data. *Bioinformatics* **30**: 3399–3401.

Mansfield J, Genin S, Magori S, Citovsky V, Sriariyanum M, Ronald P, Dow M, Verdier V, Beer SV, Machado MA, *et al.* 2012. Top 10 plant pathogenic bacteria in molecular plant pathology. *Molecular Plant Pathology* **13**: 614–629.

Matas IM, Castañeda-Ojeda MP, Aragón IM, Antúnez-Lamas M, Murillo J, Rodriquez-Palenzuela P, Lopez-Solanilla E, Ramos C. **2014**. Translocation and functional analysis of Pseudomonas savastanoi pv. savastanoi NCPPB 3335 type III secretion system effectors reveals two novel effector families of the *Pseudomonas syringae* complex. *Molecular Plant-Microbe interactions: MPMI* **27**: 424–436.

Marcelletti S, Ferrante P, Petriccione M, Firrao G, Scortichini M. **2011**. *Pseudomonas syringae* pv. *actinidiae* draft genomes comparison reveal strain-specific features involved in adaptation and virulence to *Actinidia* species. *PLoS ONE* **6**: e27297.

Martínez-García PM, Rodríguez-Palenzuela P, Arrebola E, Carrión VJ, Gutièrrez-Barranquero JA, Pèrez-García A, Ramos C, Cazorla FM, De Vicente A. **2015**. Bioinformatics analysis of the complete genome sequence of the mango tree pathogen *Pseudomonas syringae* pv. *syringae* UMAF0158 reveals traits relevant to virulence and epiphytic lifestyle. *PLoS ONE* **10**: 1–26.

Mazzaglia A, Studholme DJ, Taratufolo MC, Cai R, Almeida NF, Goodman T, Guttman DS, Vinatzer BA, Balestra GM. **2012**. *Pseudomonas syringae* pv. *actinidiae* (PSA) isolates from recent bacterial canker of kiwifruit outbreaks belong to the same genetic lineage. *PLoS ONE* **7**: 1–11.

McCann HC, Rikkerink EHA, Bertels F, Fiers M, Lu A, Rees-George J, Andersen MT, Gleave AP, Haubold B, Wohlers MW, *et al.* 2013. Genomic analysis of the kiwifruit

893 pathogen *Pseudomonas syringae* pv. *actinidiae* provides insight into the origins of an
894 emergent plant disease. *PLoS pathogens* **9**: e1003503.
895 **McCann HC, Li L, Liu Y, Li D, Pan H, Zhong C, Rikkerink EHA, Templeton MD,**
896 **Straub C, Colombi E, *et al.* 2017**. Origin and evolution of the kiwifruit canker
897 pandemic. *Genome Biology and Evolution* **9**: 932–944.
898 **Ménard M, Sutra L, Luisetti J, Prunier JP, Gardan L. 2003**. *Pseudomonas syringae* pv.
899 *avii* (pv. nov.), the causal agent of bacterial canker of wild cherries (*Prunus avium*) in
900 France. *European Journal of Plant Pathology* **109**: 565–576.
901 **de Mendiburu F. 2016**. Agricolae: Statistical procedures for agricultural research. URL
902 https://cran.r-project.org/web/packages/agricolae/index.html [accessed 28th December
903 2017]
904 **Monteil CL, Yahara K, Studholme DJ, Mageiros L, Méric G, Swingle B, Morris CE,**
905 **Vinatzer BA, Sheppard SK. 2016**. Population-genomic insights into emergence, crop-
906 adaptation, and dissemination of *Pseudomonas syringae* pathogens. *Microbial Genomics*
907 **21**: e000089.
908 **Moretti C, Cortese C, Passos da Silva D, Venturi V, Ramos C, Firrao G, Buonaurio R.**
909 **2014**. Draft genome sequence of *Pseudomonas savastanoi* pv. *savastanoi* strain DAPP-
910 PG 722, isolated in Italy from an olive plant affected by knot disease. *Genome*
911 *Announcements* **2**: e00864-14-e00864-14.
912 **Mott GA, Thakur S, Smakowska E, Wang PW, Belkhadir Y, Desveaux D, Guttman DS.**
913 **2016**. Genomic screens identify a new phytobacterial microbe-associated molecular
914 pattern and the cognate *Arabidopsis* receptor-like kinase that mediates its immune
915 elicitation. *Genome Biology* **17**: 98.
916 **Moulton J, Vivian A, Hunter P, Taylor JD. 1993**. Changes in cultivar-specificity toward
917 pea can result from transfer of plasmid RP4 and other incompatibility group P1
918 replicons to *Pseudomonas syringae* pv. *pisi*. *Journal of General Microbiology* **39**: 3149–
919 3155.
920 **Nahar K, Matsumoto I, Taguchi F, Inagaki Y, Yamamoto M, Toyoda K, Shiraishi T,**
921 **Ichinose Y, Mukaihara T. 2014**. *Ralstonia solanacearum* type III secretion system
922 effector Rip36 induces a hypersensitive response in the nonhost wild eggplant *Solanum*
923 *torvum*. *Molecular Plant Pathology* **15**: 297–303.
924 **Neale HC, Laister R, Payne J, Preston G, Jackson RW, Arnold DL. 2016**. A low
925 frequency persistent reservoir of a genomic island in a pathogen population ensures

island survival and improves pathogen fitness in a susceptible host. *Environmental Microbiology* **18**: 4144–4152.

Neale HC, Slater RT, Mayne L-M, Manoharan B, Arnold DL. **2013**. In planta induced changes in the native plasmid profile of *Pseudomonas syringae* pathover *phaseolicola* strain 1302A. *Plasmid* **70**: 420–424.

Nowell RW, Laue BE, Sharp PM, Green S. **2016**. Comparative genomics reveals genes significantly associated with woody hosts in the plant pathogen *Pseudomonas syringae*. *Molecular Plant Pathology* **17**: 1409–1424.

O'Brien HE, Thakur S, Gong Y, Fung P, Zhang J, Yuan L, Wang PW, Yong C, Scortichini M, Guttman DS. **2012**. Extensive remodeling of the *Pseudomonas syringae* pv. *avellanae* type III secretome associated with two independent host shifts onto hazelnut. *BMC microbiology* **12**: 141.

O'Brien HE, Thakur S, Guttman DS. **2011**. Evolution of plant pathogenesis in *Pseudomonas syringae*: a genomics perspective. *Annual review of phytopathology* **49**: 269–289.

Pagel M. **2004**. Detecting correlated evolution on phylogenies: A general method for the comparative analysis of discrete characters. *Proceedings of the Royal Society of London. Series B, Biological Sciences* **255**: 37–45.

Paradis E, Claude J, Strimmer K. **2004**. APE: Analyses of phylogenetics and evolution in R language. *Bioinformatics* **20**: 289–290.

Parkinson N, Bryant R, Bew J, Elphinstone J. **2011**. Rapid phylogenetic identification of members of the *Pseudomonas syringae* species complex using the *rpoD* locus. *Plant Pathology* **60**: 338–344.

Pitman AR, Jackson RW, Mansfield JW, Kaitell V, Thwaites R, Arnold DL. **2005**. Exposure to host resistance mechanisms drives evolution of bacterial virulence in plants. *Current Biology: CB* **15**: 2230–2235.

Posada D. **2008**. jModelTest: Phylogenetic model averaging. *Molecular Biology and Evolution* **25**: 1253–1256.

Press MO, Li H, Creanza N, Kramer G, Queitsch C, Sourjik V, Borenstein E. **2013**. Genome-scale co-evolutionary inference identifies functions and clients of bacterial Hsp90. *PLoS Genetics* **9**: e1003631.

Qi M, Wang D, Bradley CA, Zhao Y. **2011**. Genome sequence analyses of *Pseudomonas savastanoi* pv. *glycinea* and subtractive hybridization-based comparative genomics with nine pseudomonads. *PLoS ONE* **6**: e16451.

960 **Quevillon E, Silventoinen V, Pillai S, Harte N, Mulder N, Apweiler R, Lopez R**. **2005**.
961 InterProScan: Protein domains identifier. *Nucleic Acids Research* **33**: 116–120.
962 **R Core Team**. **2012**. *R: A language and environment for statistical computing*. Vienna,
963 Austria: R Foundation for Statistical Computing.
964 **Ravindran A, Jalan N, Yuan JS, Wang N, Gross DC**. **2015**. Comparative genomics of
965 *Pseudomonas syringae* pv. *syringae* strains B301D and HS191 and insights into
966 intrapathovar traits associated with plant pathogenesis. *Microbiology Open* **4**: 553–573.
967 **Rezaei R, Taghavi SM**. **2014**. Host specificity, pathogenicity and the presence of virulence
968 genes in Iranian strains of *Pseudomonas syringae* pv. *syringae* from different hosts.
969 *Archives of Phytopathology and Plant Protection* **47**: 2377–2391.
970 **Rodríguez-Palenzuela P, Matas IM, Murillo J, López-Solanilla E, Bardaji L, Pérez-**
971 **Martínez I, Rodríguez-Moskera ME, Penyalver R, López MM, Quesada JM, *et al.***
972 **2010**. Annotation and overview of the *Pseudomonas savastanoi* pv. *savastanoi* NCPPB
973 3335 draft genome reveals the virulence gene complement of a tumour-inducing
974 pathogen of woody hosts. *Environmental microbiology* **12**: 1604–1620.
975 **Şahin F**. **2001**. Severe outbreak of bacterial speck, caused by *Pseudomonas syringae* pv.
976 *tomato*, on field-grown tomatoes in the eastern Anatolia region of Turkey. *Plant*
977 *Pathology* **50**: 799.
978 **Sarkar SF, Gordon JS, Martin GB, Guttman DS**. **2006**. Comparative genomics of host-
979 specific virulence in *Pseudomonas syringae*. *Genetics* **174**: 1041–1056.
980 **Sawada H, Suzuki F, Matsuda I, Saitou N**. **1999**. Phylogenetic analysis of *Pseudomonas*
981 *syringae* pathovars suggests the horizontal gene transfer of argK and the evolutionary
982 stability of *hrp* gene cluster. *Journal of molecular evolution* **49**: 627–644.
983 **Sawada H, Shimizu S, Miyoshi T, Shinozaki T, Kusumoto S, Noguchi M, Naridomi T,**
984 **Kikuhara K, Kansako M, Fujikawa T, *et al.* 2015**. *Pseudomonas syringae* pv.
985 *actinidiae* biovar 3. *Japanese Journal of Phytopathology* **81**: 111–126.
986 **Sawyer S**. **1989**. Statistical tests for detecting gene conversion. *Molecular Biology and*
987 *Evolution* **6**: 526–538.
988 **Scholz-Schroeder BK, Hutchison ML, Grgurina I, Gross DC**. **2001**. The contribution of
989 syringopeptin and syringomycin to virulence of *Pseudomonas syringae* pv. *syringae*
990 strain B301D on the basis of *sypA* and *syrB1* biosynthesis mutant analysis. *Molecular*
991 *Plant-Microbe Interactions: MPMI* **14**: 336–348.

992 **Schulze-Lefert P, Panstruga R**. **2011**. A molecular evolutionary concept connecting
993 nonhost resistance, pathogen host range, and pathogen speciation. *Trends in plant*
994 *science* **16**: 117–125.
995 **Scortichini M**. **2010**. Epidemiology and predisposing factors of some major bacterial
996 diseases of stone and nut fruit trees species. *Journal of Plant Pathology* **92**: 73–78.
997 **Shafer A, Tauch A, Jager W, Kalinowski J, Thierbach G, Puhler A**. **1994**. Small
998 mobilizable multi-purpose cloning vectors derived from the *Escherichia coli* plasmids
999 pK18 and pK19: selection of defined deletions in the chromosome of *Corynebacterium*
1000 *glutamicum*. *Gene* **145**: 69–73.
1001 **Sohn KH, Zhang Y, Jones JDG**. **2009**. The *Pseudomonas syringae* effector protein,
1002 AvrRPS4, requires in planta processing and the KRVY domain to function. *Plant*
1003 *Journal* **57**: 1079–1091.
1004 **Stamatakis A**. **2014**. RAxML version 8: A tool for phylogenetic analysis and post-analysis
1005 of large phylogenies. *Bioinformatics* **30**: 1312–1313.
1006 **Staskawicz BJ, Dahlbeck D, Keen NT**. **1984**. Cloned avirulence gene of *Pseudomonas*
1007 *syringae* pv. *glycinea* determines race-specific incompatibility on *Glycine max* (L.)
1008 Merr. *Proceedings of the National Academy of Sciences of the United States of America*
1009 **81**: 6024–6028.
1010 **Thakur S, Weir BS, Guttman D**. **2016**. Phytopathogen genome announcement: Draft
1011 genome sequences of 62 *Pseudomonas syringae* type and pathotype strains. *Molecular*
1012 *Plant-Microbe Interactions* **29**: 243–246.
1013 **Vicente JG, Alves JP, Russell K, Roberts SJ**. **2004**. Identification and discrimination of
1014 *Pseudomonas syringae* isolates from wild cherry in England. *European Journal of Plant*
1015 *Pathology* **110**: 337–351.
1016 **Visnovsky SB, Fiers M, Lu A, Panda P, Taylor R, Pitman AR**. **2016**. Draft genome
1017 sequences of 18 strains of *Pseudomonas* isolated from kiwifruit plants in New Zealand
1018 and overseas. *Genome Announcements* **4**: e00061–e00016.
1019 **Walker BJ, Abeel T, Shea T, Priest M, Abouelliel A, Sakthikumar S, Cuomo CA, Zeng**
1020 **Q, Wortman J, Young SK, *et al.* 2014**. Pilon: An integrated tool for comprehensive
1021 microbial variant detection and genome assembly improvement. *PLoS ONE* **9**: e112963.
1022 **Wang Y, Li J, Hou S, Wang X, Li Y, Ren D, Chen S, Tang X, Zhou J-M**. **2010**. A
1023 *Pseudomonas syringae* ADP-ribosyltransferase inhibits Arabidopsis mitogen-activated
1024 protein kinase kinases. *The Plant cell* **22**: 2033–2044.

Warnes G, Bolker B, Bonebakker L, Gentleman R, Huber W, Liaw A, Lumley T, Maechler M, Magnusson A, Moeller S, *et al.* 2016. gplots: Various R programming tools for plotting data. URL https://cran.r-project.org/web/packages/gplots/index.html [accessed 28th December 2017]

Wu S, Lu D, Kabbage M, Wei H-L, Swingle B, Records AR, Dickman M, He P, Shan L. 2011. Bacterial effector HopF2 suppresses *Arabidopsis* innate immunity at the plasma membrane. *Molecular Plant-Microbe Interactions: MPMI* **24**: 585–593.

Xiang T, Zong N, Zou Y, Wu Y, Zhang J, Xing W, Li Y, Tang X, Zhu L, Chai J, *et al.* 2008. *Pseudomonas syringae* effector AvrPto blocks innate immunity by targeting receptor kinases. *Current Biology: CB* **18**: 74–80.

Young J. 1991. Pathogenicity and identification of the lilac pathogen, *Pseudomonas syringae* pv. *syringae* van Hall 1902. *Ann. Appl. Biol.* **118**: 283–298.

Young JM. 2010. Taxonomy of *Pseudomonas syringae*. *Journal of Plant Pathology* **92**: S1.5-S1.14.

Yu D, Yin Z, Li B, Jin Y, Ren H, Zhou J, Zhou W, Liang L, Yue J, Xu S. 2016. Gene flow, recombination, and positive selection in *Stenotrophomonas maltophilia*: Mechanisms underlying the diversity of the widespread opportunistic pathogen. *Genome* **59**: 1063–1075.

Yu G, Smith D, Zhu H, Guan Y, Lam T. 2017. ggtree: An R package for visualization and annotation of phylogenetic trees with their covariates and other associated data. *Methods in Ecology and Evolution* **8**: 28-36

Zhang J, Li W, Xiang T, Liu Z, Laluk K, Ding X, Zou Y, Gao M, Zhang X, Chen S, *et al.* 2010. Receptor-like cytoplasmic kinases integrate signaling from multiple plant immune receptors and are targeted by a *Pseudomonas syringae* effector. *Cell host & microbe* **7**: 290–301.

Zhao Y, Ma Z, Sundin GW. 2005. Comparative genomic analysis of the pPT23A plasmid family of *Pseudomonas syringae*. *Journal of Bacteriology* **187**: 2113–2126.

Zhao W, Jiang H, Tian Q, Hu J. 2015. Draft genome sequence of *Pseudomonas syringae* pv. *persicae* NCPPB 2254. **3**: 54–55.

Figure legends

Fig. 1: Core genome phylogenetic tree. Multi-locus phylogeny based on 1035 genes which represent the core genome of *P. syringae*. Strains from cherry and plum are highlighted in pink and blue respectively. Strains pathogenic to cherry (assessed in Hulin *et al.*, 2018 and Vicente *et al.*, 2004) are labelled with red circles. * indicates non-pathogenic to cherry in controlled pathogenicity tests. Phylogroups are also labelled for reference. Percentage bootstrap support values below 99% are shown for each node. The scale is nucleotide substitutions per site.

Fig. 2: Virulence gene identification. a: Heatmap of virulence gene presence and absence across *P. syringae*. The dark green squares indicate presence of a full-length T3E homologue whereas light green squares indicate that the gene is disrupted or truncated in some way. Other non-T3 secreted virulence factors are coloured in dark and light blue. Strains infecting cherry and plum are highlighted in pink and blue respectively. * indicates non-pathogenic to cherry in controlled pathogenicity tests. The cherry-pathogenic clades are illustrated via horizontal shading of cells with *Psm* R1 in blue, *Psm* R2 in light green, *Pss* in light red and *P.s* pv. *avii* in orange. Strains are ordered based on the core genome phylogenetic tree which is represented by the dendrogram. b: The total number of full-length and pseudogenised T3E genes plotted for each strain.

Fig. 3: Association of T3E evolution with cherry pathogenicity. a: Barplot showing the likelihood ratio for the correlation of each effector gene family with cherry pathogenicity based on BayesTraits analysis using the core genome phylogeny. The values are obtained from means of 100 independent runs of the program with error bars showing standard error. Those effectors that were not significantly associated with pathogenicity are coloured in grey. Coloured bars were associated with pathogenicity. GLOOME analysis revealed those significant effector genes where presence of the gene was associated with pathogenicity ($p \leq 0.05$). These are coloured in shades of blue, whilst where the significant gene was absent in cherry pathogenic clades the bar is coloured in shades of red. b: Gain and loss of BayesTraits-associated T3Es in cherry-pathogenic clades on the core genome phylogeny predicted using GLOOME (probability ≥ 0.8). For visualisation, clades within the phylogenetic tree have been collapsed with cherry pathogenic clades in pink (*Psm* R1 plum strains in blue). *Psa*: *P.s* pv. *avii*. Effectors are colour-coded based on the bar colours in A.

*: The probability of this effector being gained/lost was slightly lower than 0.8 (see Table S11 for details). c: Heatmap of presence and absence of associated effectors across *P. syringae*. This was constructed as in Fig. 2. Cherry-pathogenic strains are highlighted by pink vertical shading of columns.

Fig. 4: Horizontal gene transfer has played a key role in the evolution of cherry pathogenicity. a: Transfer of *avrD1*, *hopBB1* and *hopBF1* between different cherry-pathogenic clades based on the *P. syringae* core genome phylogeny. Strains that possess the T3E are coloured in blue, and those that are cherry-pathogenic are highlighted in red. The transfer events predicted by RANGER-DTL are shown by purple arrows. The scale-bar shows substitutions per site. b: DNA alignments of genomic regions containing these effectors. Alignments are colour-coded based on similarity where identical residues are in grey, whereas dissimilar residues appear in black. The effector gene is coloured in red, mobile element genes are in green and other CDS are in blue. Cherry-pathogenic strains are named in pink. Gene name abbreviations: ME, mobile element, Res, resolvase, Hypo, hypothetical protein gene; ISPsy4, insertion sequence, PHP, polymerase and histidinol phosphatase.

Fig. 5: Evolution of *hopAR1* in different clades of *P. syringae* containing cherry pathogens. a: Maximum-likelihood phylogenetic tree built using the nucleotide sequences of the *hopAR1* gene. Cherry and plum isolated strains are highlighted in pink and blue respectively. R1-9657* is classed as a non-pathogen of cherry. Bootstrap supports less than 100% are shown. The scale is nucleotide substitutions per site. * points to the clustering of *Psm* R2 sequences with syr2675. b: Genomic locations of the *hopAR1* gene in the three PacBio-sequenced cherry pathogens. The gene is located within prophage sequences in *Psm* R1 and R2 (see Table S13 for details), whereas in syr9097 it is on a genomic island adjacent to a tRNA gene. Effector genes are coloured in red, other CDS in blue, phage genes predicted by PHASTER and mobile element genes are in green, tRNA genes in pink and genomic islands predicted (GI14 in *Psm* R2 and GI23 in *Pss*) in light blue. # Indicates that *hopBK1* is a pseudogene in this strain. The end of predicted prophage sequences is denoted with a dashed green line. c: Alignment of the region surrounding the *hopAR1* gene in several strains. The blue box indicates the region in d. All sequences share an upstream tRNA-Thr gene in pink. The phage region in the bean pathogens syr2676 and syr2675 (shortened due to it being at the end of a contig) and *Psm* R2-leaf are highlighted in a green box. Other mobile elements

are also coloured in green. The *hopAR1* gene is coloured in red and outlined with a red box. All strains with the phage sequences and syr9097 also contain *attL* and *attR* repeats which are putative insertion sites. Additional closely related phylogroup 2 (P2) strains (USA011, syr1212, syrB728A) which lack the *hopAR1* gene are included for comparison. Homologous regions are highlighted in yellow to show regions of similarity between P2 strains. d: Close-up alignment of the genomic regions surrounding the *hopAR1* gene in strains of P2, *Psm* R2, *P.s* pv. *amygdali* and *P.s* pv. *avii* that share homology in the surrounding regions. tRNA genes are in pink, phage/mobile element genes are in green, CDS in blue and the *hopAR1* T3E gene is coloured red and highlighted with a red box. Alignments are colour-coded based on similarity where identical residues are in grey, whereas dissimilar residues appear in black. * The syr2675 *hopAR1* gene is similar to *Psm* R2 sequences and also has homologous phage sequences upstream.

Fig. 6: Genomic islands characteristic of cherry pathogens are found across *P. syringae*. The heatmap shows the presence and absence of the genomic islands identified in the PacBio sequenced pathogenic strains of (a) *Psm* R1, (b) *Psm* R2 and (c) *Pss* across the *P. syringae* complex. Dark green squares indicate that the full-length GI is putatively present. Light green squares are where the GI was predicted to be partially present. The names of strains that infect cherry and plum are coloured in pink and blue, respectively. Strains that were not pathogenic but were isolated from cherry are marked with an asterisk. The different phylogroups 1,2 and 3 are delimited by black borders. Pink arrows point to GIs that contain T3E or phytotoxin genes. *Psm*R1 GIs - 1: coronatine biosynthesis genes, 2: *hopF3*, 3: *hopA1*, 4: *hopAT1*, 5: *hopBL2*, 6: *hopAO2*, 7: *hopAY1*, *Psm* R2 GIs - 8: *hopAT1*, 9: *hopD1*, 10: *hopX1*, 11: *hopAR1*, 12: *hopE1*, 13: *hopAE1*, 14: *avrB2*, 15: *hopAZ1*, 16: *hopAF1*, 17: *hopH1*, *Pss* GIs – 18: *hopAR1*, 19: *avrRpm1*, 20: *hopBE1*. Full details are in Tables S14-S16.

Fig. 7: Identification of avirulence factors activating ETI in cherry. a: Boxplot of an initial ten-day population count analysis of cherry pathogens (R1-5244, R2-leaf and syr9644) transconjugants expressing candidate avirulence genes. The data presented are based on one experiment, with three leaf replicates and three nested technical replicates (n=9). Controls included the wildtype strain, a strain containing the empty pBBR1MCS-5 vector and a Δ*hrpA* deletion mutant (for R1-5244 and R2-leaf). A separate ANOVA was performed for each cherry pathogen (R1-5244, R2-leaf and syr9644) and the Tukey-HSD significance groups (p=0.05, confidence level: 0.95) for each strain are presented above each boxplot. b: Boxplot

of ten-day population counts of cherry pathogens (R1-5244, R2-leaf and syr9644) expressing different HopAB alleles and HopC1. The data presented are based on three independent experiments (n=27). Tukey-HSD significance groups (p=0.05, confidence level: 0.95) are presented above each boxplot. c: Symptom development of R1-5244, R2-leaf, syr9644 transconjugants. Mean symptom score values are presented and represent two independent experiments (n=6). Error bars show standard error above and below the mean. Symptoms assessed as degree of browning of the infiltration site, 1: some browning, 2:< 50%, 3:>50%, 4: 100% of the infiltrated area brown. Analysis was based on Area Under Disease Progress Curves values (0-48 h), see Tables S25-S26. An ANOVA was performed on AUDPC values, with * indicating significantly different from the empty vector (EV) control. d: Symptom development over time on a leaf inoculated with R1-5244 transconjugants. HPI: Hours post inoculation. The order of strains: 1: EV, 2: *hopAB1*, 3: *hopAB2*, 4: *hopAB3*, 5: *hopC1*. Arrows indicate the first appearance of symptoms associated with each strain and are coloured based on the graph in c. e: Alignment of the DNA region surrounding *hopAB1* in *Psm* R1 strains. Grey indicates sequence identity whereas black indicates divergence. The effector genes are coloured in red, whereas other CDS are in blue and putative mobile element genes are in green. * indicates the location of *hopAB1* in R1-5300, whilst the upstream effectors are *hopQ1*, *hopD1* and *hopR1*. The second alignment shows the *hopAB3* gene of *Psm* R2 and close out-groups. * The *hopAB3* gene has been truncated due to a GG insertion leading to a frameshift in *Psm* R2, whilst in *P.s* pv. *avii* (avii3846) there is a deletion at the end of the gene. f: Diagrams showing the location of key domains in the HopAB3 protein including the Pto-interaction domain (PID), BAK1-interacting domain (BAK1) and E3 ubiquitin ligase (E3). The E3 domain is lost completely from the *Psm* R2 protein whereas in avii3846 the beginning of this domain is lost. The PID domain was not detected in the cherry pathogen sequences. g: Boxplot of ten-day population counts of R1-5244 trans-conjugants expressing three different *hopAB* alleles, including $hopAB3_{R2\text{-}leaf}$ and *hopC1*. The data presented are based on two independent experiments (n=18). Tukey-HSD significance groups (p=0.05, confidence level: 0.95) are presented above each boxplot. h: Representative image of symptoms 10 dpi with the different R1-5244 transconjugants when inoculated at a low level to observe pathogenicity. Arrows point to pathogenic symptoms in the strain expressing $hopAB3_{R2\text{-}leaf}$ and the EV strain, colour-coded as in g. ANOVA tables for all statistical analyses are presented in Tables S17-S25.

Fig. 8: Model highlighting genomic events that have led to the evolution of pathogenicity towards cherry. a: The core genome phylogeny is presented. Scale bar shows substitutions per site. For visualisation, clades within the phylogenetic tree have been collapsed with clades containing cherry pathogens in pink (*Psm* R1 plum strains in blue). Examples of cherry pathogens within each clade of phylogroup 2 are named. HGT events predicted using phylogenetic analysis and RANGER-DTL are shown. b: The key gains and losses of associated virulence genes in strains pathogenic to cherry are described. Where a gene is present but not necessarily predicted to be gained in this clade, it is shown with a plus sign, whilst the use of the words gain or loss specifically denotes results based on GLOOME analysis. *: The probability of this effector being gained/lost predicted using GLOOME was slightly lower than 0.8 (see Table S11 for details). For *Pss* strains within P2, present toxin biosynthesis gene clusters are shown as dots for comparison. Orange: mangotoxin, blue: syringopeptin, green: syringolin, pink: syringomycin.

Table 1: List of bacterial strains used in this study. Pathovar designation, phylogroup, isolation information, cherry pathogenicity (reference for when tested and Nt for not tested) and reference for publication of genome sequence are included. NCBI accession numbers are also listed. Strains in bold were considered pathogenic in cherry. # The pathogenic status of MAFF302280 on cherry is debated. This strain is reported to be the pathotype strain of *P.s* pv. *morsprunorum* (Sawada *et al.*, 1999), so is assumed to be equivalent to CFBP 2351, NCPPB2995, ICMP5795 and LMG5075. The strain NCPPB2995 was reported to be potentially non-pathogenic (Gardan *et al.*, 1999). In comparison, the 'same' strain LMG5075 tested positive for pathogenicity in a recent publication (Gilbert *et al.*, 2009). There is no definite link showing that MAFF302280 is the same strain as the others listed as it is not linked to them in online databases (http://www.straininfo.net/) or taxonomy-focused publications (Bull *et al.*, 2010). It is assumed to be putatively pathogenic in this study due to its close relatedness to other *Psm* R2 strains, however further pathogenicity tests would be required to fully confirm this.

Strain	Pathovar	Race	PG	Isolation source	Isolator	*Prunus* cv.	Sequenced	Pathogenicity tested on cherry (*Prunus avium*)	BioProject/accession
avii5271	***avii***		**1**	***Prunus avium***	**Garrett, 1990, UK**	**Wild cherry**	**This study**	**Vicente *et al.*, 2004**	**NBAO00000000**
R1-5270	***morsprunorum***	**1**	**3**	***Prunus avium***	**Garrett, 1990, UK**	**Wild cherry**	**This study**	**Vicente *et al.*, 2004**	**NBAN00000000**
R2-7968A	***morsprunorum***	**2**	**1**	***Prunus avium***	**Vicente, 2000, UK**	**Wild cherry**	**This study**	**Vicente *et al.*, 2004**	**NBAI00000000**
R2-9095	***morsprunorum***	**2**	**1**	***Prunus avium***	**Roberts, 2010, UK**	**Wild cherry**	**This study**	**M. Hulin, pers. obs.**	**MLED00000000**
syr5264	***syringae***		**2**	***Prunus avium***	**Garrett, 1990 UK**	**Wild cherry**	**This study**	**Vicente *et al.*, 2004**	**NBAQ00000000**
syr5275	***syringae***		**2**	***Prunus avium***	**Garrett, 1990 UK**	**Wild cherry**	**This study**	**Vicente *et al.*, 2004**	**NBAP00000000**
syr7928A	***syringae***		**2**	***Prunus avium***	**Vicente, 2000, UK**	**Wild cherry**	**This study**	**Vicente *et al.*, 2004**	**NBAL00000000**
syr8094A	***syringae***		**2**	***Prunus avium***	**Vicente, 2001, UK**	**Wild cherry**	**This study**	**Vicente *et al.*, 2004**	**NBAK00000000**
Ps-7928C	unknown		2	*Prunus avium*	Vicente, 2000, UK	Wild cherry	This study	Vicente *et al.*, 2004	NBAM00000000

Ps-7969	unknown		2	*Prunus avium*	Vicente, 2000, UK	Wild cherry	This study	Vicente *et al.*, 2004	NBAJ00000000
syr2675	*syringae*		2	*Phaseolus vulgaris*	1965, Kenya		This study	This study	MLEX00000000
syr2676	*syringae*		2	*Phaseolus vulgaris*	1990, Lesotho		This study	This study	MLEY00000000
syr2682	*syringae*		2	*Phaseolus vulgaris*	1990, Lesotho		This study	This study	MLFA00000000
syr3023	*syringae*		2	*Syringa vulgaris*	1950, UK		This study	This study	MLFD00000000
syr100	*syringae*		2	*Phaseolus lunatus*	1962, Kenya		This study	This study	MLEV00000000
R1-5244	***morsprunorum***	**1**	**3**	***Prunus avium***	**Cross, 1960, UK**	**Unknown**	**Hulin *et al.*, 2018**	**Hulin *et al.*, 2018**	**MLEB00000000**
R1-5300	*morsprunorum*	1	3	*Prunus domestica*	Prunier, UK	Victoria	Hulin *et al.*, 2018	Hulin *et al.*, 2018	MLEN00000000
R1-9326	*morsprunorum*	1	3	*Prunus domestica*	Roberts, 2011, UK	Victoria	Hulin *et al.*, 2018	Hulin *et al.*, 2018	MLEO00000000
R1-9629	*morsprunorum*	1	3	*Prunus domestica*	Roberts, 2012, UK	Victoria	Hulin *et al.*, 2018	Hulin *et al.*, 2018	MLEP00000000
R1-9646	***morsprunorum***	**1**	**3**	***Prunus avium***	**Roberts, 2012, UK**	**Stella**	**Hulin *et al.*, 2018**	**Hulin *et al.*, 2018**	**MLEE00000000**
R1-9657	*morsprunorum*	1	3	*Prunus avium*	Roberts, 2012, UK	Kiku-Shidare	Hulin *et al.*, 2018	Hulin *et al.*, 2018	MLEF00000000
R2-5255	***morsprunorum***	**2**	**1**	***Prunus avium***	**Prunier, UK**	**Napoleon**	**Hulin *et al.*, 2018**	**Hulin *et al.*, 2018**	**MLEC00000000**
R2-5260	***morsprunorum***	**2**	**1**	***Prunus avium***	**Garrett, UK**	**Roundel**	**Hulin *et al.*, 2018**	**Hulin *et al.*, 2018**	**MLEG00000000**
R2-leaf	***morsprunorum***	**2**	**1**	***Prunus avium***	**Hulin, 2014, UK**	**Napoleon**	**Hulin *et al.*, 2018**	**Hulin *et al.*, 2018**	**MLEH00000000**
R2-SC214	***morsprunorum***	**2**	**1**	***Prunus avium***	**Roberts, 1983, UK**	**Wild cherry**	**Hulin *et al.*, 2018**	**Hulin *et al.*, 2018**	**MLEI00000000**
syr9097	***syringae***		**2**	***Prunus avium***	**Roberts, 2010, UK**	**Unknown**	**Hulin *et al.*, 2018**	**Hulin *et al.*, 2018**	**MLEJ00000000**
syr9293	***syringae***		**2**	***Prunus domestica***	**Roberts, 2011, UK**	**Victoria**	**Hulin *et al.*, 2018**	**Hulin *et al.*, 2018**	**MLEQ00000000**
syr9630	***syringae***		**2**	***Prunus domestica***	**Roberts, 2012, UK**	**Victoria**	**Hulin *et al.*, 2018**	**Hulin *et al.*, 2018**	**MLER00000000**
syr9644	***syringae***		**2**	***Prunus avium***	**Roberts, 2012, UK**	**Stella**	**Hulin *et al.*, 2018**	**Hulin *et al.*, 2018**	**MLEK00000000**
syr9654	***syringae***		**2**	***Prunus domestica***	**Roberts, 2012, UK**	**Victoria**	**Hulin *et al.*, 2018**	**Hulin *et al.*, 2018**	**MLES00000000**
syr9656	***syringae***		**2**	***Prunus avium***	**Roberts, 2012, UK**	**Kiku-Shidare**	**Hulin *et al.*, 2018**	**Hulin *et al.*, 2018**	**MLEM00000000**

syr9659	***syringae***		**2**	***Prunus avium***	**Roberts, 2012, UK**	**Kiku-Shidare**	**Hulin *et al.*, 2018**	**Hulin *et al.*, 2018**	**MLEL00000000**
Ps-9643	unknown		1	*Prunus domestica*	Roberts, 2012, UK	Victoria	Hulin *et al.*, 2018	Hulin *et al.*, 2018	MLET00000000
avii3846	***avii***		**1**	***Prunus avium***	**1991, France**	**Wild cherry**	**Nowell *et al.*, 2016**	**Ménard *et al.*, 2003**	**LIIJ00000000**
R1-2341	***morsprunorum***	**1**	**3**	***Prunus cerasus***	**1988, Hungary**	**Unknown**	**Nowell *et al.*, 2016**	**Nowell *et al.*, 2016**	**LIIB00000000**
R1-5269	***morsprunorum***	**1**	**3**	***Prunus cerasus***	**Garrett, 1990, UK**	**Wild cherry**	**Nowell *et al.*, 2016**	**Vicente *et al.*, 2004**	**LIHZ00000000**
R2-5261	***morsprunorum***	**2**	**1**	***Prunus avium***	**Garrett, UK**	**Roundel**	**Nowell *et al.*, 2016**	**Vicente *et al.*, 2004**	**LIIA00000000**
R2-302280	***morsprunorum***		**1**	***Prunus domestica***	**USA**	**Unknown**	**Baltrus *et al.*, 2011**	**Gilbert *et al.*, 2009[#]**	**AEAE00000000**
syr2339	***syringae***		**2**	***Prunus avium***	**1984, Hungary**	**Unknown**	**Nowell *et al.*, 2016**	**Nowell *et al.*, 2016**	**LIHU00000000**
syr7872	***syringae***		**2**	***Prunus domestica***	**Lewis, 2000, UK**	**Opal**	**Nowell *et al.*, 2016**	**Vicente *et al.*, 2004**	**LIHS00000000**
syr7924	***syringae***		**2**	***Prunus avium***	**Vicente, 2000, UK**	**Wild cherry**	**Nowell *et al.*, 2016**	**Vicente *et al.*, 2004**	**LIHR00000000**
acer302273	*aceris*		2	*Acer* sp.	USA		Baltrus *et al.*, 2011	Nt	AEAO00000000
acti18884	*actinidiae*		1	*Actinidia deliciosa*	2010, NZ		McCann *et al.*, 2013	Nt	AOKO00000000
acti19073	*actinidiae*		1	*Actinidia deliciosa*	1998, Korea		McCann *et al.*, 2013	Nt	AOJR00000000
acti212056	*actinidiae*		1	*Actinidia deliciosa*	2012, Japan		Sawada *et al.*, 2014	Nt	BBWG00000000
acti302091	*actinidiae*		1	*Actinidia deliciosa*	1984, Japan		Baltrus *et al.*, 2011	Nt	AEAL00000000
actiCRAFRU	*actinidiae*		1	*Actinidia deliciosa*	2010, Italy		Butler *et al.*, 2013	Nt	ANGD00000000
actiNCPPB3871	*actinidiae*		1	*Actinidia deliciosa*	1992, Italy		Marceletti *et al.*, 2011	Nt	ANGD00000000
aes089323	*aesculi*		3	*Aesculus hippocastanum*	India, 1980		Baltrus *et al.*, 2011	Nt	AEAD00000000
aes2250	*aesculi*		3	*Aesculus hippocastanum*	2008, UK		Green *et al.*, 2010	Nt	ACXT00000000
aes3681	*aesculi*		3	*Aesculus hippocastanum*	1969, India		Green *et al.*, 2010	Nt	ACXS00000000
amy3205	*amygdali*		3	*Prunus dulcis*	1967, Greece		Bartoli *et al.*, 2015b	Nt	JYHB00000000
amyICMP3918	*amygdali*		3	*Prunus dulcis*	Panagopoulos, 1967, Greece		Thakur *et al.*, 2016	Nt	LJPQ00000000
avelBP631	*avellanae*		1	*Corylus avellana*	1976, Greece		O'Brien *et al.*, 2012	Hulin *et al.*, 2018	AKBS00000000
avelVe037	*avellanae*		2	*Corylus avellana*	1990, Italy		O'Brien *et al.*, 2012	Nt	AKCJ00000000

BRIP34876	unknown	2	*Hordeum vulgar*	1971, Australia	Gardiner *et al.*, 2013	Nt	AMXK00000000
castCFBP4217	*castaneae*	3	*Castanea crenata*	1977, Japan	Nowell *et al.*, 2016	Nt	LIIH00000000
CC1416	unknown	1	Epilithon	USA	Baltrus *et al.*, 2014	Nt	AVEP00000000
CC1544	unknown	1	Lake water	France	Baltrus *et al.*, 2014	Nt	AVEI00000000
CC1559	unknown	1	Snow	France	Baltrus *et al.*, 2014	Nt	AVEG00000000
CC94	unknown	2	*Cantaloupe*	France	Baltrus *et al.*, 2014	Nt	AVEA00000000
cera6109	*cerasicola*	3	*Prunus yedoensis*	1995, Japan	Nowell *et al.*, 2016	Nt	LIIG00000000
ceraICMP17524	*cerasicola*	3	*Prunus yedoensis*	Japan	Thakur *et al.*, 2016	Nt	LJQA00000000
ciccICMP5710	*ciccaronei*	3	*Ceratonia siliqua*	Italy	Thakur *et al.*, 2016	Nt	LJPY00000000
cunnICMP11894	*cunninghamiae*	3	*Cunninghamia lanceolata*	China	Thakur *et al.*, 2016	Nt	LJQE00000000
daphICMP9757	*daphniphylli*	3	*Daphniphyllum teijsmannii*	Japan	Thakur *et al.*, 2016	Nt	LJQF00000000
delphi569	*delphinii*	1	Delphinium sp.	NZ	Thakur *et al.*, 2016	Nt	LJQH00000000
dendro3226	*dendropanacis*	3	Dendropanax trifidus	1979, Japan	Bartoli *et al.*, 2015b	Nt	JYHG00000000
dendro4219	*dendropanacis*	3	Dendropanax trifidus	1981, Japan	Bartoli *et al.*, 2015b	Nt	JYHD00000000
dendro9150	*dendropanacis*	3	Dendropanax trifidus	Japan	Thakur *et al.*, 2016	Nt	LJQG00000000
erio4455	eriobotryae	3	*Eriobotrya japonica*	USA	Thakur *et al.*, 2016	Nt	LJQI00000000
glyR4	*glycinea*	3	*Glycine max*	Cross, 1960, USA	Qi *et al.*, 2011	Nt	AEGH00000000
ICMP19498	unknown	3	*Actinidia deliciosa*	2010, NZ	Visnovsky *et al.*, 2016	Nt	LKCH00000000
lach301315	*lachrymans*	3	*Cucumis sativus*	Japan	Baltrus *et al.*, 2011	Nt	AEAF00000000
lach302278	*lachrymans*	1	*Cucumis sativus*	USA	Baltrus *et al.*, 2011	Nt	AEAM00000000
lapsaICMP3947	*lapsa*	2	*Zea* sp.	Unknown	Thakur *et al.*, 2016	Nt	LJQQ00000000
meli6289	*meliae*	3	*Melia azedarach*	Japan	Thakur *et al.*, 2016	Nt	LJQT00000000
morsU7805	*morsprunorum*	3	*Prunus mume*	Unknown	Mott *et al.*, 2016	Nt	LGLQ00000000
myriAZ8448	*myricae*	3	*Myrica rubra*	Japan	Thakur *et al.*, 2016	Nt	LGLA00000000
neriiICMP16943	*savastanoi*	3	*Olea europea*	Spain	Thakur *et al.*, 2016	Nt	LJQW00000000

paniLMG2367	*panici*	2	*Panicum miliaceum*	Unknown	Liu *et al.*, 2012	Nt	ALAC00000000
papu1754	*papulans*	2	*Malus sylvestris*	1973, Canada	Nowell *et al.*, 2016	Nt	JYHI00000000
persNCPPB2254	*persicae*	1	*Prunus persica*	1972, France	Zhao *et al.*, 2015	Nt	LAZV00000000
photICMP7840	*photiniae*	3	*Photinia glabra*	Japan	Thakur *et al.*, 2016	Nt	LJQO00000000
pisiPP1	*pisi*	2	*Pisum sativum*	Japan	Baltrus *et al.*, 2014b	Nt	AUZR00000000
phas1448a	*phaseolicola*	3	*Phaseolus vulgaris*	Teverson, 1965, Ethiopia	Joardar *et al.*, 2005	Hulin *et al.*, 2018	CP000058
rhapCFBP4220	*rhaphiolepidis*	3	*Rhaphiolepis umbellata*	1980, Japan	Nowell *et al.*, 2016	Nt	LIHV00000000
RMA1	unknown	1	*Aquilegia vulgaris*	Jackson, 2012, UK	Hulin *et al.*, 2018	Hulin *et al.*, 2018	MLEU00000000
sava3335	*savastanoi*	3	*Olea europea*	Stead, France	Rodriguez-Palenzuela *et al.*, 2010	Nt	ADMI00000000
sava4352	*savastanoi*	3	*Olea europea*	Yugoslavia	Thakur *et al.*, 2016	Nt	LGKR00000000
savaDAPP-PG722	*savastanoi*	3	*Olea europea*	Italy	Moretti *et al.*, 2014	Nt	JOJV00000000
savaPseNe107	*savastanoi*	3	*Olea europea*	Balestra, Nepal	bartoli *et al.*, 2015b	Nt	JYHF00000000
soliICMP16925	*solidagae*	2	*Solidago altissima*	Japan	Thakur *et al.*, 2016	Nt	JYHF00000000
syr1212	*syringae*	2	*Pisum sativum*	UK	Baltrus *et al.*, 2014	This study	AVCR00000000
syr2340	*syringae*	2	*Pyrus* sp.	1985, Hungary	Nowell *et al.*, 2016	Nt	LIHT00000000
syr41a	*syringae*	2	*Prunus armeniaca*	2011, France	Bartoli *et al.*, 2015b	Nt	JYHJ00000000
syrB301D	*syringae*	2	*Pyrus communis*	Garrett, 1959, UK	Ravindran *et al.*, 2015	Nt	CP005969
syrB64	*syringae*	2	*Triticum aestivum*	Wilcoxson, USA	Dudnik and Dudler 2013	Nt	ANZF00000000
syrB728a	*syringae*	2	*Phaseolus vulgaris*	1987, USA	Feil *et al.*, 2005	This study	CP000075
syrHS191	*syringae*	2	*Panicum miliaceum*	Hayward, Australia, 1969	Ravindran *et al.*, 2015	Nt	CP006256
syrUMAF0158	*syringae*	2	*Mangifera indica*	Cazorla, 2010, Spain	Martínez-García *et al.*, 2015	Nt	CP005970
thea3923	*theae*	1	*Camelia sinensis*	1974, Japan	Mazzaglia *et al.*, 2012	Nt	AGNN00000000
tomaDC3000	*tomato*	1	*Solanum*	1960, UK	Buell *et al.*, 2003	Nt	AE016853

			lycopersicum				
tomaT1	*tomato*	1	*Solanum lycopersicum*	1986, Canada	Almeida *et al*., 2009	Nt	ABSM00000000
UB303	unknown	2	Lake water	France	Baltrus *et al*., 2014	Nt	AVDZ00000000
ulmiICMP3962	*ulmi*	3	*Ulmus* sp.	Yugoslavia	Thakur *et al*., 2016	Nt	LJRQ00000000
USA007	unknown	1	Stream water	USA	Baltrus *et al*., 2014	Nt	AVDY00000000
USA011	unknown	1	Stream water	USA	Baltrus *et al*., 2014	Nt	AVDX00000000

Table 2: Assembly statistics for all strains in this study and by Hulin *et al.* (2018). Cherry pathogens are in bold. N50: The weighted median contig size in the assembly. Features: The number of protein encoding and RNA sequences in the annotated genome.

Assembly	Sequencing	Reference	No. contigs	Plasmids	Total length	GC %	N50	Average coverage	Features
R1-5270	**Illumina**	**This study**	**185**	**3**	**6258313**	**58.10**	**202152**	**134**	**5770**
R1-5244	**Illumina**	**Hulin *et al.*, 2018**	**198**	**4**	**6302385**	**58.08**	**227422**	**265**	**5810**
R1-5300	Illumina	Hulin *et al.*, 2018	201	4	6342586	57.88	142021	180	5844
R1-9326	Illumina	Hulin *et al.*, 2018	268	4	6353636	57.91	142021	81	5874
R1-9629	Illumina	Hulin *et al.*, 2018	216	3	6341664	57.94	142021	172	5856
R1-9646	**Illumina**	**Hulin *et al.*, 2018**	**171**	**3**	**6302776**	**58.03**	**235429**	**180**	**5801**
R1-9657	Illumina	Hulin *et al.*, 2018	191	4	6317852	57.91	145272	158	5848
R2-5255	**Illumina**	**Hulin *et al.*, 2018**	**206**	**2**	**6448834**	**58.38**	**102760**	**112**	**5966**
R2-7968A	**Illumina**	**This study**	**278**	**6**	**6498711**	**58.42**	**91262**	**134**	**6016**
R2-5260	**Illumina**	**Hulin *et al.*, 2018**	**223**	**3**	**6495620**	**58.41**	**101794**	**458**	**5995**
R2-9095	**Illumina**	**This study**	**304**	**2**	**6418849**	**58.48**	**92453**	**100**	**5887**
R2-leaf	**Illumina**	**Hulin *et al.*, 2018**	**203**	**5**	**6366714**	**58.48**	**100658**	**180**	**5846**
R2-SC214	**Illumina**	**Hulin *et al.*, 2018**	**203**	**3**	**6253818**	**58.56**	**108341**	**180**	**5747**
avii5271	**Illumina**	**This study**	**352**	**6**	**6243644**	**58.56**	**56064**	**127**	**5809**
Ps-9643	Illumina	Hulin *et al.*, 2018	58	1	5937102	58.78	243355	212	5386
syr9097	**Illumina**	**Hulin *et al.*, 2018**	**66**	**0**	**5892389**	**59.35**	**316078**	**158**	**5117**
syr9293	**Illumina**	**Hulin *et al.*, 2018**	**73**	**0**	**6135031**	**58.84**	**557853**	**196**	**5302**
syr9630	**Illumina**	**Hulin *et al.*, 2018**	**57**	**0**	**5940819**	**59.33**	**347701**	**206**	**5175**
syr9644	**Illumina**	**Hulin *et al.*, 2018**	**75**	**1**	**6173193**	**59.13**	**251053**	**208**	**5334**
syr9654	**Illumina**	**Hulin *et al.*, 2018**	**49**	**0**	**5941610**	**59.37**	**245023**	**147**	**5148**
syr9656	**Illumina**	**Hulin *et al.*, 2018**	**39**	**0**	**5980728**	**59.10**	**1007808**	**205**	**5184**
syr9659	**Illumina**	**Hulin *et al.*, 2018**	**51**	**0**	**5943090**	**59.37**	**235830**	**116**	**5148**

syr5264	**Illumina**	**This study**	**59**	**0**	**6029896**	**59.08**	**380149**	**114**	**5314**
syr5275	**Illumina**	**This study**	**64**	**1**	**5994091**	**59.30**	**371492**	**145**	**5207**
syr7928A	**Illumina**	**This study**	**59**	**1**	**6129363**	**59.26**	**371492**	**141**	**5338**
syr8094A	**Illumina**	**This study**	**71**	**0**	**5942438**	**59.33**	**265238**	**106**	**5184**
syr7928C	Illumina	This study	49	1	5994455	59.17	325175	124	5318
syr7969	Illumina	This study	92	0	6185932	59.01	164374	151	5476
RMA1	Illumina	Hulin *et al.*, 2018	95	1	6306889	58.73	187448	320	5825
syr100	Illumina	This study	23	0	5872916	59.33	893822	83	5140
syr2675	Illumina	This study	65	0	5994384	59.34	227612	83	5177
syr2676	Illumina	This study	90	1	6158476	59.30	259660	78	5387
syr2682	Illumina	This study	185	1	6259099	59.21	242212	84	5405
syr3023	Illumina	This study	228	0	6203212	58.90	456738	88	5365
R1-5244	**PacBio**	**This study**	**5**	**4**	**6445963**	**58.05**	**6109228**	**82**	**6024**
R2-leaf	**PacBio**	**This study**	**6**	**5**	**6576340**	**58.41**	**6242845**	**141**	**6093**
syr9097	**PacBio**	**This study**	**1**	**0**	**5929959**	**59.30**	**5929959**	**100**	**5147**
R1-5300	MinION	This study	6	4	6645601	57.87	5688034	100	6449

Table 3: List of effectors in genomes sequenced using PacBio/Minion methods. Effectors are listed in order of appearance on each assembly contig (labelled as chromosomal or plasmid). Where effectors could be considered as linked (within 10kb of each other) they are underlined. * indicates effectors within the conserved effector locus. #: Effector gene is disrupted and is labelled as a pseudogene.

R1-5244	**Contig**	**Length**	**Effectors**
Chromosome	tig0	6109228	*hopAZ1*, *hopA2*#, *avrE1*, *hopM1*#, *hopAA1*# *, *hopZ4*, *hopAT1*, *hopQ1*, *hopD1*, *hopR1*, *hopF4*, *hopBL2*, *hopAV1*, *hopAO2*#, *hopAY1*, *hopF3*, *hopAS1*, *hopI1*, *hopAE1*, *hopAF1-2*, *hopAU1*, *hopAH1*, *hopV1*, *hopAR1*, *hopBK1*#
Plasmid	tig3	168854	*hopAF1-1*, *hopBF1*, *avrD1*, *avrRpm2*, *hopBD1*
Plasmid	tig4	81536	*hopA1*
Plasmid	tig5	45535	-
Plasmid	tig6	40810	-
R1-5300	**Contig**	**Length**	**Effectors**
Chromosome	tig0	5688034	*hopV1*, *hopAZ1*, *avrA1*, *hopQ1-2*, *hopA2*#, *avrE1*, *hopM1*#, *hopAA1**, *hopAB1*, *hopQ1*, *hopD1*, *hopR1*, *hopAO2*#, *avrRpm2*, *avrPto1*, *hopAS1*, *hopAT1*#, *hopBL2*#, *hopI1*, *hopAE1*, *hopAF1-2*, *hopF3*, *hopAY1*#, *hopAU1*, *hopAH1*
Chromosome	tig75	697453	*hopW1*, *hopBK1*#, *hopAR1*
Plasmid	tig46	52059	-
Plasmid	tig65	47809	*hopX1*, *hopBB1*, *hopG1*
Plasmid	tig84	57689	*hopAO1*#
Plasmid	tig113	102557	*avrD1*
R2-leaf	**Contig**	**Length**	**Effectors**
Chromosome	tig0	6242845	*hopY1*, *hopAS1*, *hopAT1*, *hopH1*, *hopF4*, *hopW1*, *hopR1*, *hopAG1*#, *hopAH1-2*, *hopAI1*, *hopN1*, *hopAA1*#, *hopM1*, *avrE1**, *hopF2*, *hopE1*, *hopA2*, *hopAH1-1*, *hopAH1-1*, *hopAB3*#, *avrRps4*, *hopS2*, *hopI1*, *hopAR1*
Plasmid	tig5	102862	*hopAO1*#, *hopAZ1*, *hopAY1*
Plasmid	tig4	97840	*hopD1*#, *hopAU1*
Plasmid	tig6	69519	*hopAF1-1*, *hopBF1*
Plasmid	tig8	42783	*hopBB1*, *hopBD1*
Plasmid	tig9	20491	*avrB2*, *hopX1*
syr9097	**Contig**	**Length**	**Effectors**

Chromosome	tig0	5929959	*hopAG1, hopAH1, hopA1I, avrRpm1, hopAR1, hopI1, hopAE1, hopBE1, hopAF1, hopAH1, hopAW1#, hopH1, hopA2, avrE1, hopM1, hopAA1**

Table 4: List of putative horizontal gene transfer events that have occurred between *Prunus*-infecting clades within *P. syringae*. Where the effector gene is present in the PacBio- or Minion-sequenced strains its chromosomal or plasmid location is indicated. #: Effector gene is disrupted and is labelled as a pseudogene.

Effector	Putative transfers	Region	Plasmid location	Predicted in RangerDTL
avrD1	R1/R2/*P.s* pv. *avii*	Plasmid	tig3 (R1-5244)	Y
avrRps4[#]	R2/*P.s* pv. *avii*	Next to cluster of mobile elements	-	Y
hopAF1	R1/R2/*P.s* pv *avii*	Plasmid	tig3 (R1-5244), tig6 (R2)	Y
hopAO1	R2/*P.s* pv *avii*/R1-5300	Plasmid	tig5(R2), tig84 (R1-5300)	N
hopAT1	R1/R2	Genomic island	-	N
hopAU1	R2/*P.s* pv. *avii*	Plasmid	tig4 (R2)	Y
hopAY1	R2/*P.s* pv. *avii*	Plasmid	tig5 (R2)	Y
hopBB1	R1/R2/*P.s* pv. *avii*	Plasmid	tig8 (R2), tig65 (R1-5300)	Y
hopBD1	R2/*P.s* pv. *avii*	Plasmid	tig3 (R1-5244), tig8 (R2)	Y
hopBF1	R1/R2/*P.s* pv. *avii*	Plasmid	tig3 (R1-5244), tig6 (R2)	Y
hopD1	R2/*P.s* pv. *avii*	Plasmid	tig4(R2)	N
hopO1	R2/*P.s* pv. *avii*	Next to cluster of mobile elements (next to *hopT1*)	-	Y
hopT1	R2/*P.s* pv. *avii*	Next to cluster of mobile elements (next to *hopO1*)	-	Y

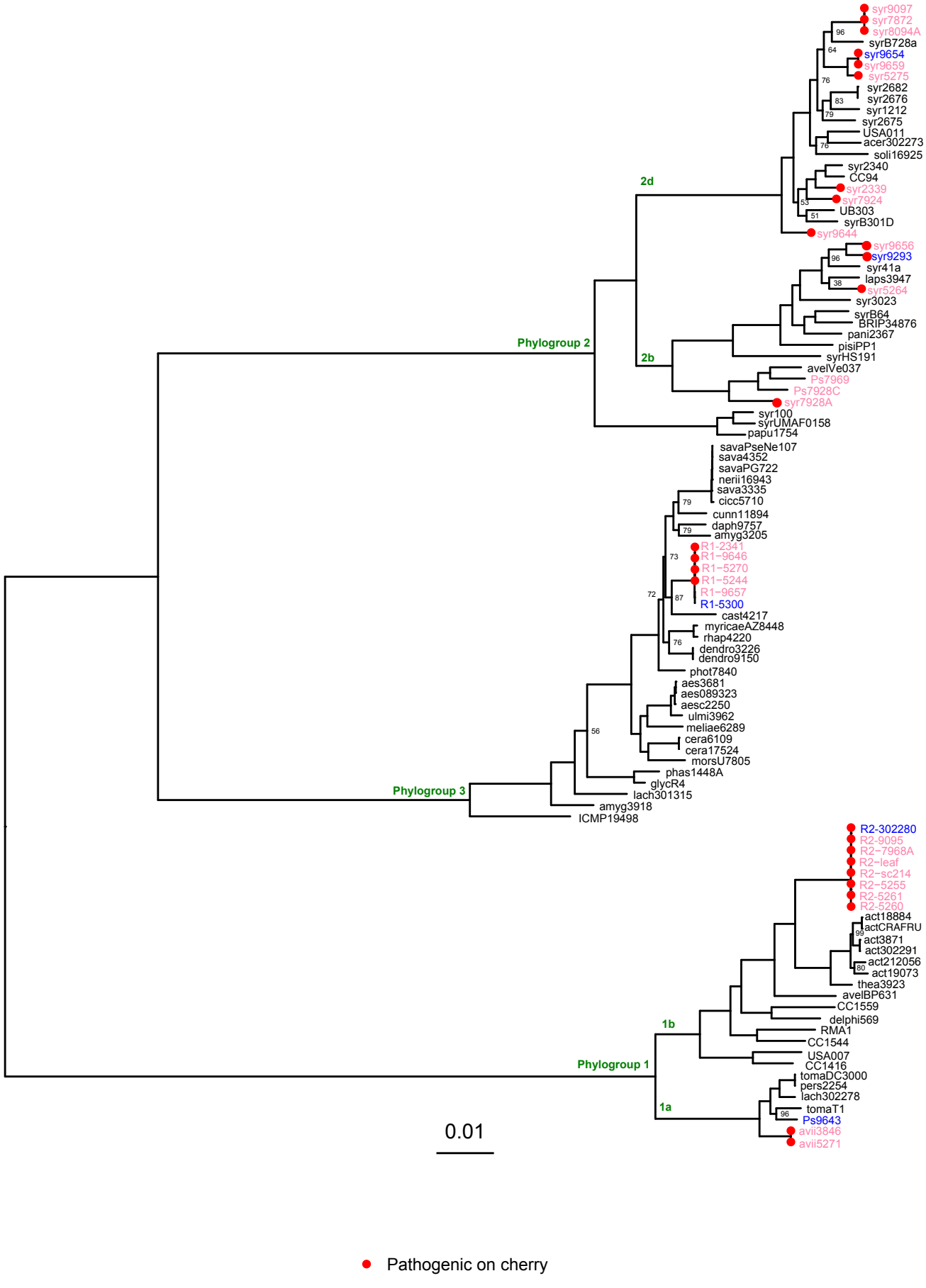
syr9097
syr7872
syr8094A
syrB728a
syr9654
syr9659
syr5275
syr2682
syr2676
syr1212
syr2675
USA011
acer302273
soli16925
syr2340
CC94
syr2339
syr7924
UB303
syrB301D
syr9644
2d
syr9656
syr9293
syr41a
laps3947
syr5264
syr3023
syrB64
BRIP34876
pani2367
pisiPP1
syrHS191
avelVe037
Ps7969
Ps7928C
syr7928A
2b
Phylogroup 2
syr100
syrUMAF0158
papu1754
savaPseNe107
sava4352
savaPG722
nerii16943
sava3335
cicc5710
cunn11894
daph9757
amyg3205
R1-2341
R1−9646
R1−5270
R1−5244
R1−9657
R1-5300
cast4217
myricaeAZ8448
rhap4220
dendro3226
dendro9150
phot7840
aes3681
aes089323
aesc2250
ulmi3962
meliae6289
cera6109
cera17524
morsU7805
phas1448A
glycR4
lach301315
amyg3918
ICMP19498
Phylogroup 3
R2-302280
R2-9095
R2−7968A
R2−leaf
R2−sc214
R2−5255
R2-5261
R2-5260
act18884
actCRAFRU
act3871
act302291
act212056
act19073
thea3923
avelBP631
CC1559
delphi569
RMA1
CC1544
USA007
CC1416
tomaDC3000
pers2254
lach302278
tomaT1
Ps9643
avii3846
avii5271
1b
1a
Phylogroup 1
0.01
Pathogenic on cherry

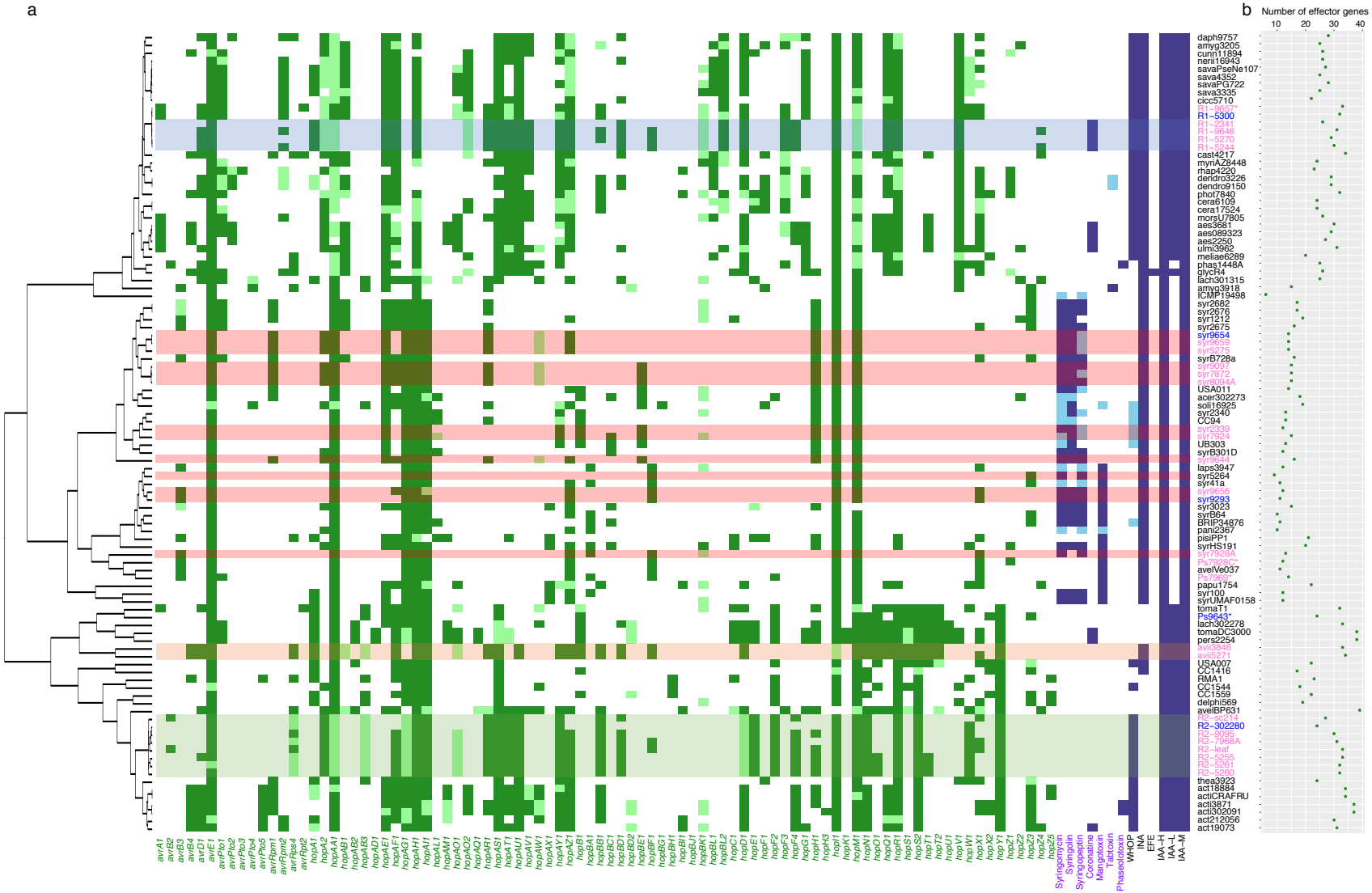
a
b
Number of effector genes
10
20
30
40
daph9757
amyg3205
cunin11894
nerii18943
savaPseNe107
sava4352
savaPG722
sava3335
cicc5710
R1–9457*
R1–5300
R1–2341
R1–9646
R1–5270
R1–5244
cast4217
myriAZ8448
rhap4220
deridro3226
dendro9150
phot7840
cera6109
cera17524
morsU7805
aes3681
aes089323
aes2250
ulmi3962
meliae6289
phas1448A
glycR4
lach301315
amyg3918
ICMP19498
syr2682
syr2676
syr1212
syr2675
syr9654
syr9639
syr5278
syrB728a
syr9637
syr7872
cit9015A
USA011
acer302273
soli16925
syr2340
CC94
syr2339
syr7924
UB303
syrB301D
syr9641
laps3947
syr5264
syr41a
syr9636
syr9293
syr3023
syrB64
BRIP34876
pani2367
pisPP1
syrHS191
syr7928A
Ps79029C*
aveVe037
Ps7969*
papu1754
syr100
syrUMAF0158
tomaT1
Ps9643*
lach302278
tomaDC3000
pers2254
avi3949
avi8271
USA007
CC1416
RMA1
CC1544
CC1559
delphi569
aveIBP631
R2–8274
R2–302280
R2–9095
R2–7968A
R2–leaf
R2–5255
R2–5261
R2–5260
thea3923
act18884
actICRAFRU
acti3871
acti302091
act212056
act19073
avrA1
avrB2
avrB3
avrB4
avrD1
avrE1
avrPto1
avrPto2
avrPto3
avrPtoA
avrPtoB
avrRpm1
avrRpm2
avrRps4
avrRpt2
hopA1
hopA2
hopAA1
hopAB1
hopAB2
hopAB3
hopAD1
hopAE1
hopAF1
hopAG1
hopAH1
hopAI1
hopAL1
hopAM1
hopAO1
hopAO2
hopAQ1
hopAR1
hopAS1
hopAT1
hopAU1
hopAV1
hopAW1
hopAX1
hopAY1
hopAZ1
hopB1
hopBA1
hopBB1
hopBC1
hopBD1
hopBD2
hopBE1
hopBF1
hopBG1
hopBH1
hopBJ1
hopBK1
hopBL1
hopBL2
hopC1
hopD1
hopE1
hopF1
hopF2
hopF3
hopF4
hopG1
hopH1
hopH3
hopI1
hopK1
hopM1
hopN1
hopO1
hopQ1
hopR1
hopS1
hopS2
hopT1
hopT2
hopU1
hopV1
hopW1
hopX1
hopX2
hopY1
hopZ1
hopZ2
hopZ3
hopZ4
hopZ5
Syringomycin
Syringotoxin
Syringopeptin
Coronatine
Mangotoxin
Tabtoxin
Phaseolotoxin
WHOP
INA
EFE
IAA–H
IAA–L
IAA–M

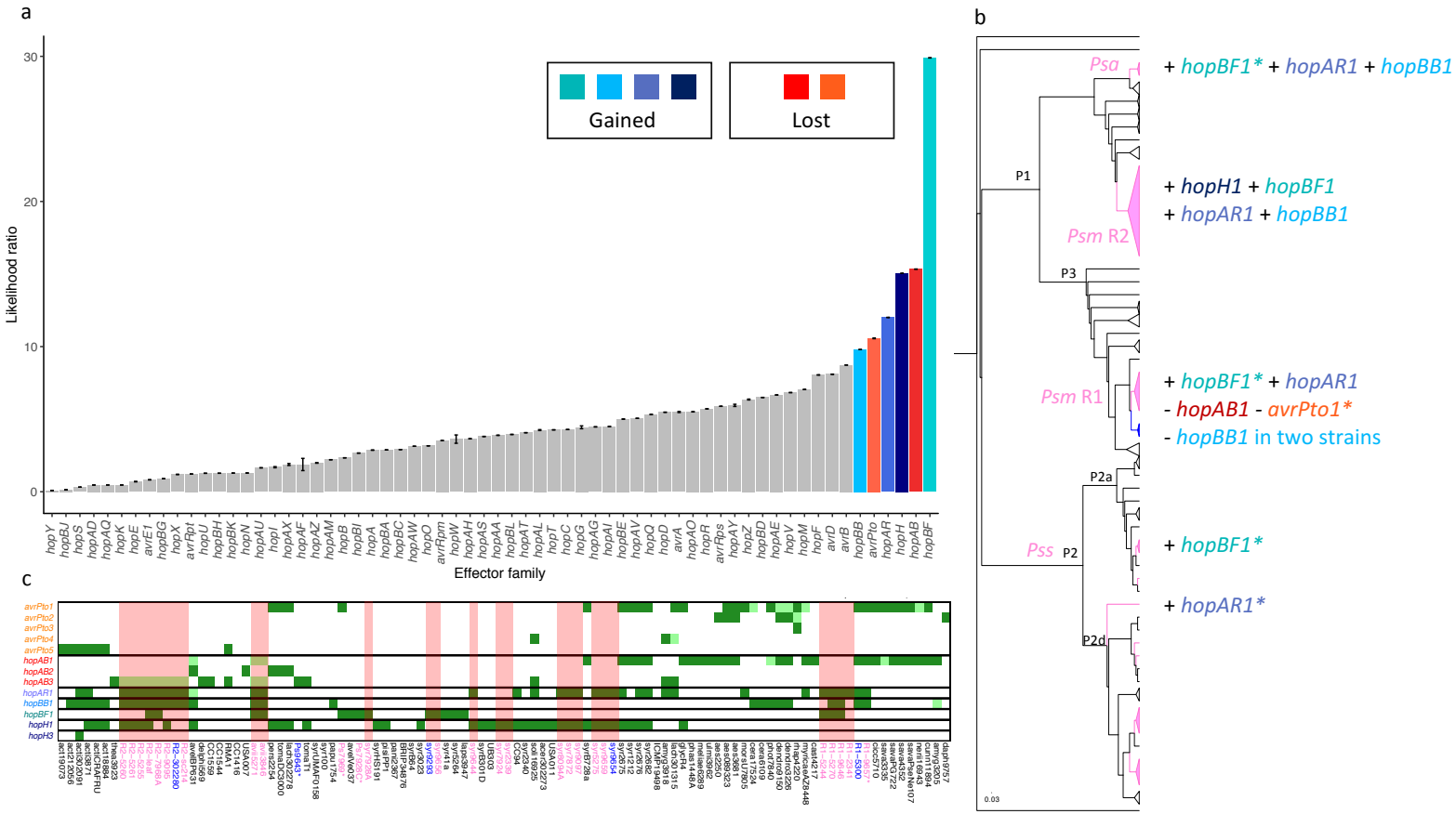
a
b
c
Likelihood ratio
Gained
Lost
Effector family
Psa
Psm R2
Psm R1
Pss
P1
P2
P2a
P2d
P3
+ hopBF1* + hopAR1 + hopBB1
+ hopH1 + hopBF1
+ hopAR1 + hopBB1
+ hopBF1* + hopAR1
- hopAB1 - avrPto1*
- hopBB1 in two strains
+ hopBF1*
+ hopAR1*

a

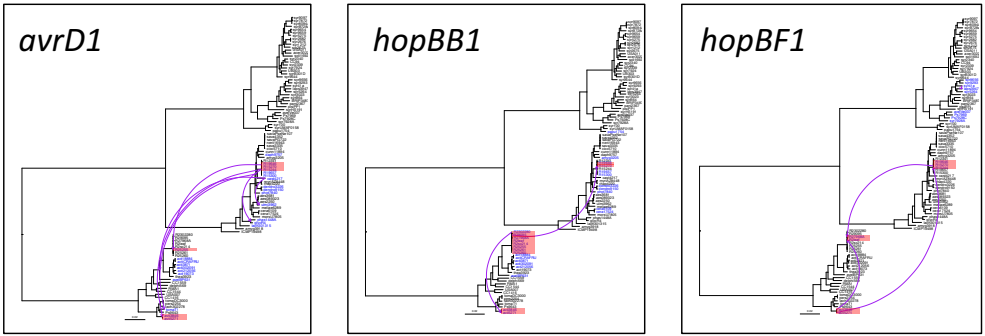
avrD1
hopBB1
hopBF1

b

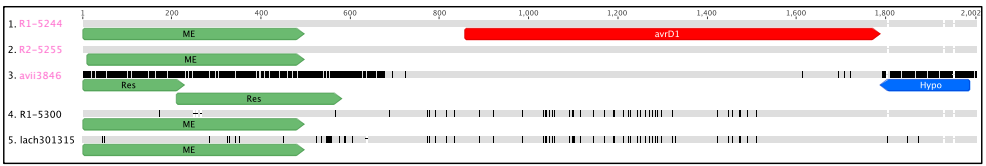
1. R1-5244
2. R2-5255
3. avii3846
4. R1-5300
5. lach301315
ME
avrD1
Res
Hypo

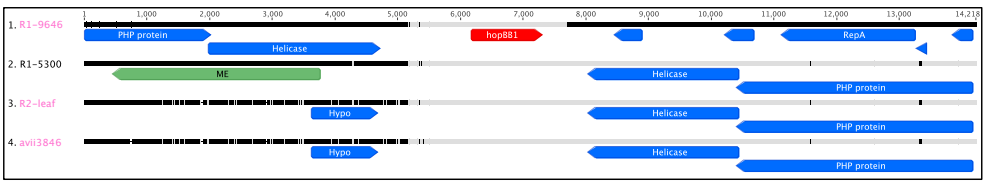
1. R1-9646
2. R1-5300
3. R2-leaf
4. avii3846
PHP protein
Helicase
hopBB1
RepA
ME
Hypo

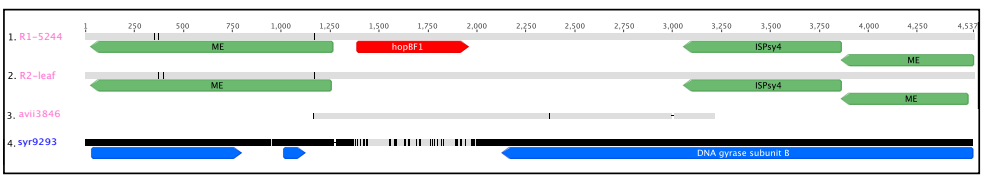
1. R1-5244
2. R2-leaf
3. avii3846
4. syr9293
ME
hopBF1
ISPsy4
DNA gyrase subunit B

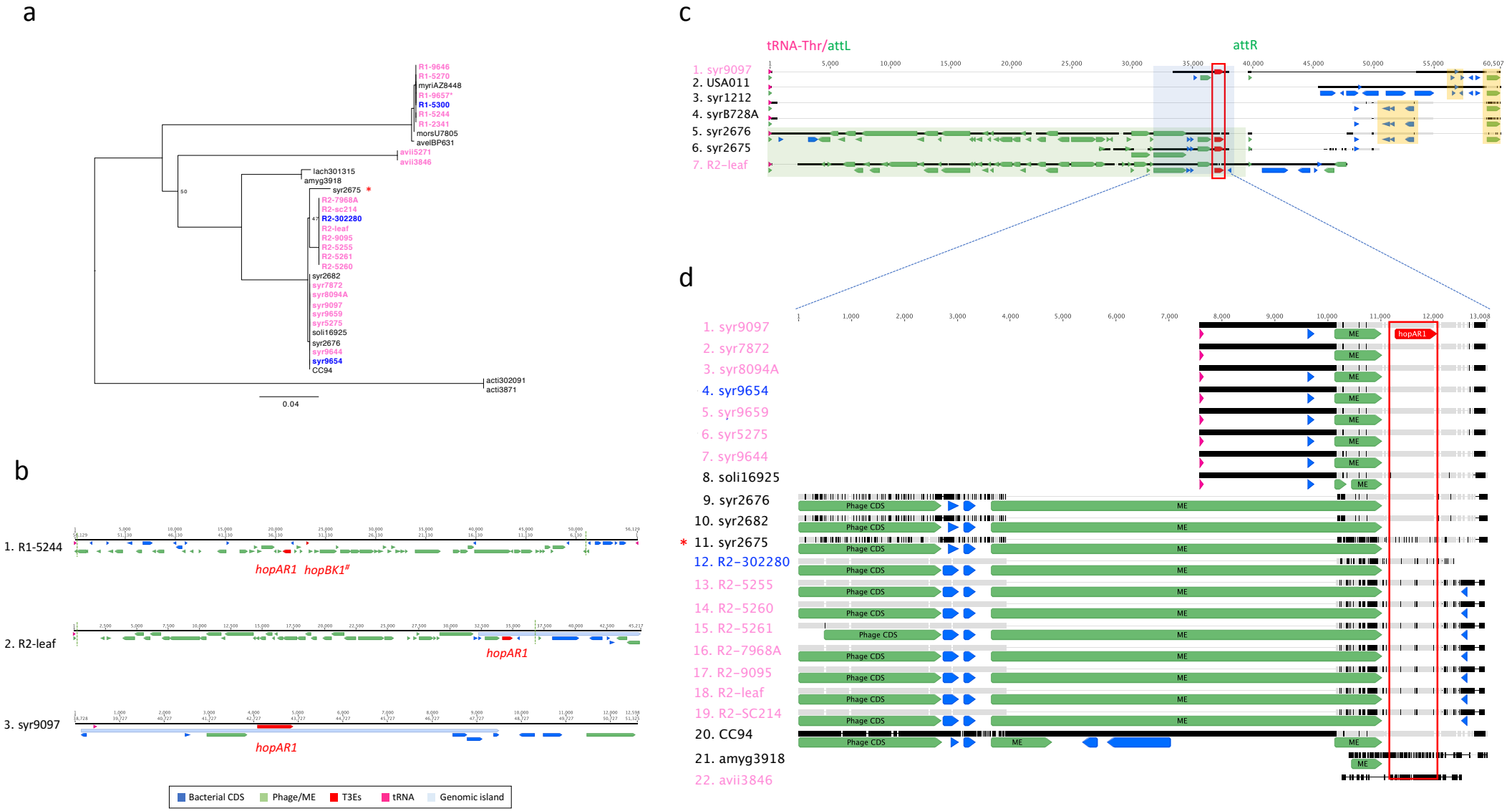
a
R1-9646
R1-5270
myriAZ8448
R1-9657*
R1-5300
R1-5244
R1-2341
morsU7805
avelBP631
avii5271
avii3846
lach301315
amyg3918
syr2675 *
R2-7968A
R2-sc214
R2-302280
R2-leaf
R2-9095
R2-5255
R2-5261
R2-5260
syr2682
syr7872
syr8094A
syr9097
syr9659
syr5275
soli16925
syr2676
syr9644
syr9654
CC94
acti302091
acti3871
50
47
0.04
b
1. R1-5244
hopAR1 hopBK1#
2. R2-leaf
hopAR1
3. syr9097
hopAR1
Bacterial CDS
Phage/ME
T3Es
tRNA
Genomic island
c
tRNA-Thr/attL
attR
1. syr9097
2. USA011
3. syr1212
4. syrB728A
5. syr2676
6. syr2675
7. R2-leaf
d
1. syr9097
2. syr7872
3. syr8094A
4. syr9654
5. syr9659
6. syr5275
7. syr9644
8. soli16925
9. syr2676
10. syr2682
* 11. syr2675
12. R2-302280
13. R2-5255
14. R2-5260
15. R2-5261
16. R2-7968A
17. R2-9095
18. R2-leaf
19. R2-SC214
20. CC94
21. amyg3918
22. avii3846
hopAR1
ME
Phage CDS

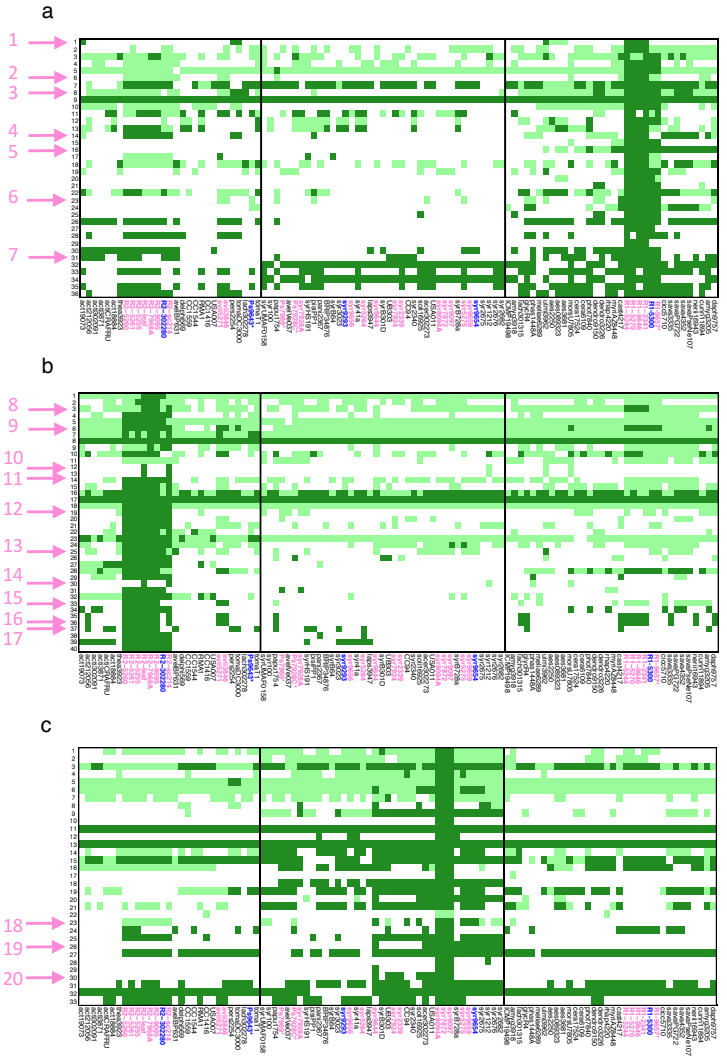
a
1
2
3
4
5
6
7
b
8
9
10
11
12
13
14
15
16
17
c
18
19
20

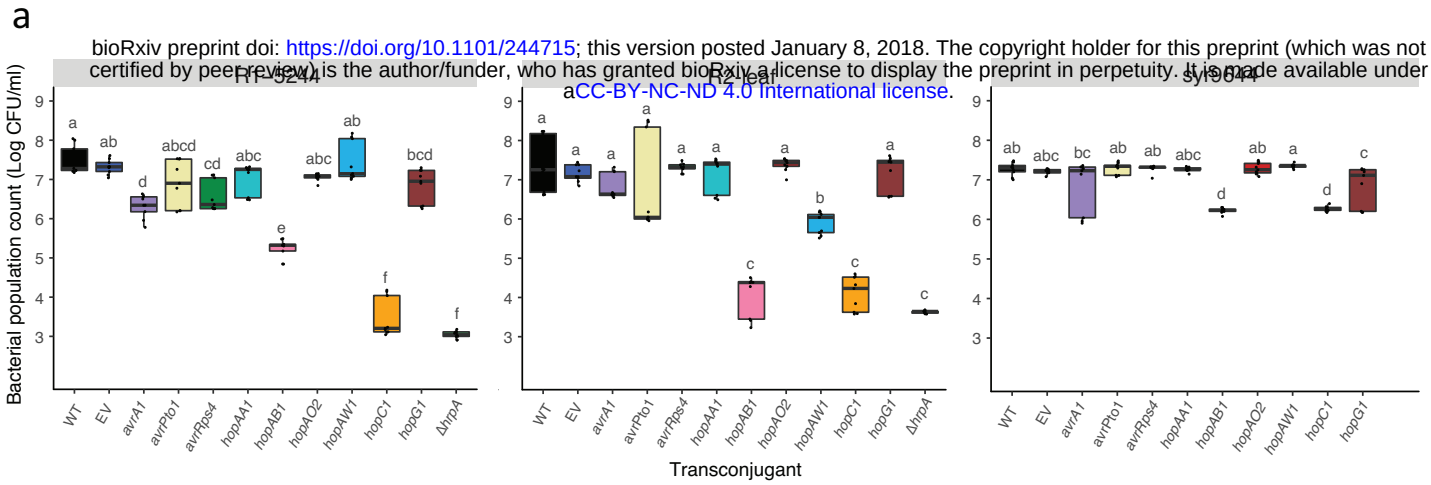

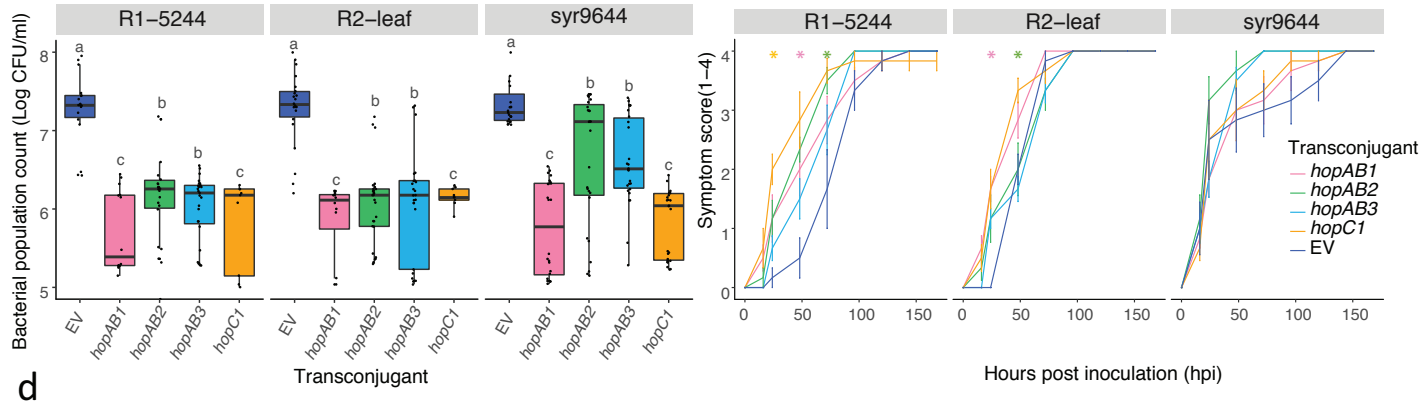

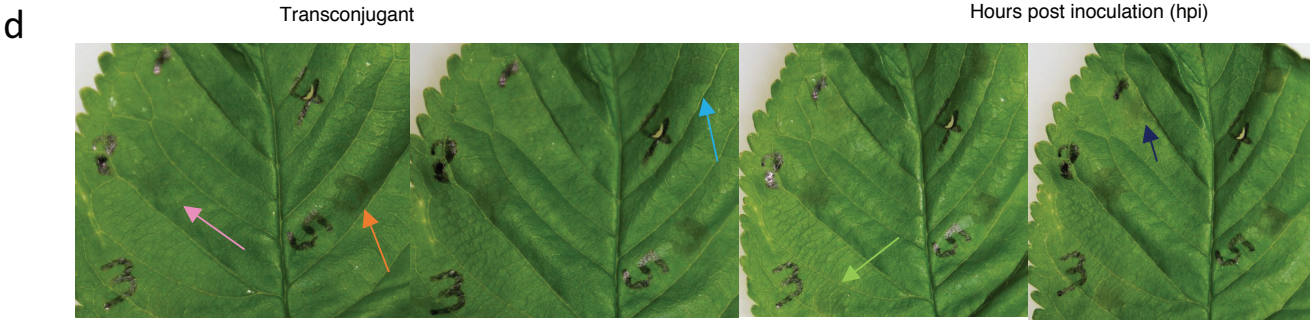

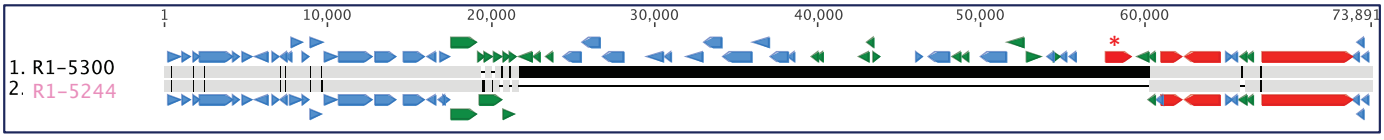

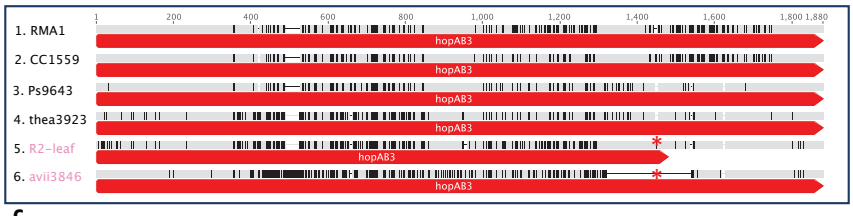

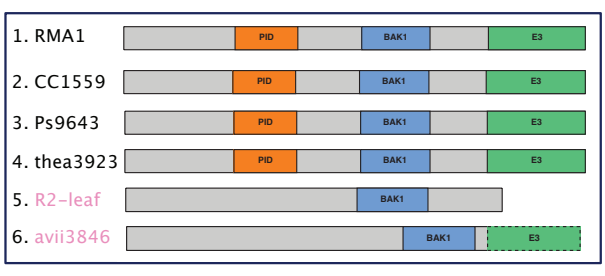

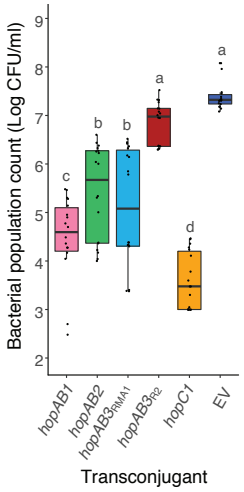

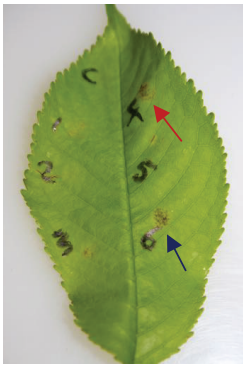

a

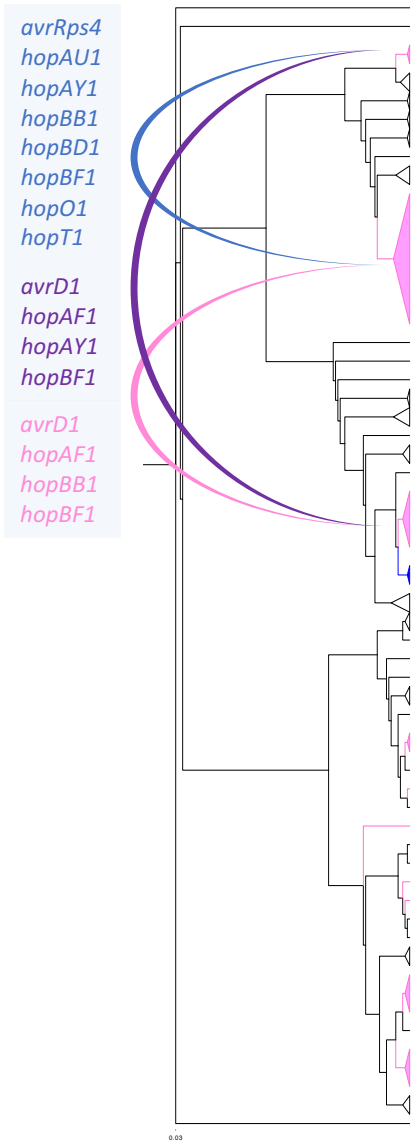

b

P1 (*P.s* pv. *avii*)	Gain of *hopBF1**, *hopAR1*, *hopBB1* Truncation of *hopAB1*, *hopAB3*
P1 (*Psm* R2)	Gain *hopH1*, *hopBF1*, *hopAR1*, *hopBB1* Truncation of *hopAB3*
P3 (*Psm* R1)	Gain *hopAR1*, *hopBF1**, cor+ Loss *hopAB1*
P2b (syr9656)	Gain of *hopBF1**
P2b (syr7928A)	*hopBF1+*
P2d (syr9644)	Gain of *hopAR1**, *hopH1+*
P2d (syr2339)	*hopH1+*, *catABC+*
P2d (syr9097)	*hopAR1+*, *hopH1+*
P2d (syr9654)	*hopAR1+*, *hopH1+*